論文 / 著書情報
Article / Book Information

題目(和文)	
Title(English)	Controlled release and immobilization of insulin-like growth factor for design of bioactive materials
著者(和文)	YunHeo
Author(English)	Yun Heo
出典(和文)	学位:博士(工学), 学位授与機関:東京工業大学, 報告番号:甲第11339号, 授与年月日:2019年12月31日, 学位の種別:課程博士, 審査員:小畠 英理,上田 宏,西山 伸宏,田巻 孝敬,三重 正和
Citation(English)	Degree:Doctor (Engineering), Conferring organization: Tokyo Institute of Technology, Report number:甲第11339号, Conferred date:2019/12/31, Degree Type:Course doctor, Examiner:,,,,
学位種別(和文)	博士論文
Type(English)	Doctoral Thesis

Controlled release and immobilization of insulin-like growth factor for design of bioactive materials

Yun Heo

Department of environmental chemistry and engineering

Tokyo Institute of Technology

2019

Table of Contents

ABSTRACT 1

List of Abbreviations 3

CHAPTER 1 GENERAL INTRODUCTION 5

1.1 Growth factors 6

1.2 Biomaterials 8

1.3 Combination of growth factors for biomaterials 10

1.3.1 Controlled release 11

1.3.2 Immobilization 12

1.4 Insulin-like growth factor (IGF) 13

1.5 Applications of IGF 15

1.6 This thesis 16

1.7 References 18

CHAPTER 2 CONTROLLED RELEASE OF IGF 29

2.1 Introduction 30

2.2 Materials and methods 31

2.2.1 Materials 31

2.2.2 Preparation of photo-curable alginate 32

2.2.3 Photo-curing of F-Alginate 34

2.2.4 Viscoelasticity measurement 34

2.2.5 Incorporation of molecules and release profile 35
2.2.6 Cell culture 35
2.2.7 Cell assay 36
2.2.8 Statistical analysis 36
2.3 Results and discussion 37
2.3.1 Characterization of F-Alginate 37
2.3.2 Photo-curing of F-Alginate 42
2.3.3 Viscoelastic property of alginate hydrogel 43
2.3.4 Release profile of F-Alginate 45
2.3.5 Cytotoxicity of photo-sensitizers 48
2.3.6 Released IGF effect on cell growth 51
2.4 Conclusion 53
2.5 References 54
CHAPTER 3 IMMOBILIZATION OF IGF 62
3.1 Introduction 63
3.2 Materials and methods 64
3.2.1 Materials 64
3.2.2 Preparation of IGF-DOPA 65
3.2.3 Binding assay 66
3.2.4 Biological activity of immobilized IGF-DOPA 66

3.3 Results and discussion 69

3.3.1 Preparation of IGF-DOPA 69

3.3.2 Binding assay 72

3.3.3 Biological activity of immobilized IGF-DOPA 73

3.4 Conclusion 76

3.5 References 77

CHAPTER 4 CONCLUSIONS 81

4.1 Summary 82

4.2 Future directions 83

4.2.1 Approach for efficient delivery of growth factors 84

4.2.2 Combination of growth factors 85

4.3 Conclusions and perspectives 83

Acknowledgments 87

List of Publications 88

ABSTRACT

Growth factors are included in cell proliferation and differentiation, and various growth factors have been developed. However, growth factors, because of their short biological half-life and lack of continuous stability, require biomaterials as drug delivery systems to be more effective. Therefore, growth factors have been used with biomaterials to promote cell growth and differentiation. Among the various growth factors, insulin-like growth factor-1 (IGF-1) has been reported as a therapeutic factor for improving the proliferation of cells and promoting osteogenic differentiation by implants.

In this thesis, two types of biomaterials are described for controlled release and immobilization of IGF-1.

Regarding controlled-release IGF-1, visible light-reactive alginate was prepared by coupling with furfurylamine. The prepared furfuryl-alginate (F-Alginate) formed gel in the presence of a photosensitizer, such as Rose Bengal or riboflavin, under visible light irradiation. Rapid gelation was observed in the group with high furan content. When the formed gel was measured by a rheometer, the F-Alginate showed high storage modulus G', which was comparable to that of the conventional Ca^{2+}-induced gelation. The release rate of encapsulated substances depended on their molecular weights. The higher was the molecular weight of encapsulated dextran, the slower was the observed release. These release behaviors were comparable to Ca^{2+}-induced gel. Cell growth was enhanced in response to the released IGF-1 and was prolonged by sustained IGF-1 release from high-molecular-weight F-Alginate hydrogel.

For the immobilization of IGF-1 on biomaterials, bioinspired method was employed. Underwater adhesive proteins have inspired the design of various functional materials. Herein, one of the key amino acids in the adhesive proteins, 3,4-dihydroxyphenylalanine, was incorporated into a growth factor polypeptide, IGF-1, to add adhesiveness for immobilization. The IGF-1 derivative adhered to various substrates involving organic and inorganic materials and enhanced the cell proliferation and bone differentiation properties of osteoblast cells. This improvement was attributed to a long-lasting cell signal transduction triggered by the bound IGF-DOPA without internalization.

List of Abbreviations

Insulin-like growth facor-1	IGF-1
Furfuryl alginate	F-Alginate
Ca^{2+}-induced alginate	C-Alginate
3,4-Dihydroxyphenylalanine	DOPA
Bone morphogenetic protein	BMP
Nerve growth factor	NGF
Fibroblast growth factor	FGF
Vascular endothelial growth factor	VEGF
Epidermal growth factor	EGF
Transforming growth factor	TGF
1-Ethyl-3-(3-dimethylaminopropyl) carbodiimide Hydrochloride	EDC
N-hydroxysuccinimide	NHS
Fluorescein isothiocyanate	FITC
Enzyme linked immunosorbent assay	ELISA
Layer by layer	LbL
Extracellular matrix	ECM

Phosphate-buffered saline	PBS
Infrared	IR
Dulbecco’s modified Eagle’s medium	DMEM
Minimum essential medium Eagle - alpha modification	MEMα
Fetal bovine serum	FBS
Polystyrene	PS
Titanium	Ti

CHAPTER 1

GENERAL INTRODUCTION

1.1 Growth factors

Growth factors are involved in cell growth, proliferation, and differentiation, and various growth factors have been identified[1, 2]. These growth factors bind to specific receptors and perform their respective functions; in addition, they act as cell signaling molecules[3, 4]. In the early days, although growth factors were discovered and reported, their separation and purification was difficult[5, 6]. However, the development of recombinant protein engineering technology has enabled effective isolation and purification of growth factors[7-9].

In particular, since tissues and organs require the action of numerous growth factors, tissue regeneration research using these growth factors is being actively performed[10, 11]. However, in tissue regeneration studies, these growth factors were found to require appropriate biomaterials for drug delivery to be more effective due to their short biological half-life, lack of continuous stability, and selective tissue compatibility[12-14]. Growth factors can be used together with biomaterials as a carrier in tissue engineering to promote the growth and differentiation of cells, thereby achieving effective tissue regeneration. In addition, proper biomaterials for biological tissue regeneration[15] and the introduction of an appropriate drug delivery system for growth factors are also important[16-18].

The following are among the various types of growth factors known: BMP[19] (bone morphogenetic protein), NGF[20] (nerve growth factor), FGF[21] (fibroblast growth factor), IGF[22] (insulin-like growth factor), VEGF[23] (vascular endothelial growth factor), EGF[24] (epidermal growth factor), and TGF[25] (transforming growth factor) (Table 1-1).

Table 1-1. Types and functions of growth factors.

Growth factors	Functions
Bone morphogenetic protein (BMP)	Proliferation and differentiation of bone cells
Nerve growth factor (NGF)	Proliferation and differentiation of nerve cell
Fibroblast growth factor (FGF)	Growth, proliferation and differentiation of cells (Fibroblasts, epithelial cells)
Insulin-like growth factor (IGF)	Cell proliferation and inhibition of cell apoptosis
Vascular endothelial growth factor (VEGF)	Proliferation and differentiation of epithelial cells
Epidermal growth factor (EGF)	Growth, proliferation and differentiation of cells (Epithelial cell)
Transforming growth factor (TGF)	Enhancement of wound healing Proliferation and differentiation of bone-forming cells

1.2 Biomaterials

Various biomaterials have been developed for medical applications. Biomaterials are made from natural or artificial raw materials for regenerating or replacing damaged tissues of the body[26, 27]. Techniques have been devised for the application of biomaterials, such as regenerative medicine, controlled drug delivery, and tissue engineering and remodeling. For example, the three-dimensional scaffold has been used to generate a cartilage tissue from stem cells; this tissue can be implanted in the body[28]. Some reports have shown an elegant application of biodegradable material for tissue remodeling using biomaterials to recover the function of a pulmonary artery[29]. Furthermore, the bio-absorbable fibers can effectively release drug came from angioplasty[30]. It has been demonstrated that drug-eluting stents using biodegradable polymer reduced the risk of stent thrombosis[31]. Owing to the biological and physicochemical properties of nanoparticles, they have gained considerable attention among researches in wound healing applications[32].

Biomaterials for medical purposes basically require several properties[33-35] (Table 1–2). They should be safe and non-toxic to the human body after use. In addition, since they are used in the body, they should be biocompatible with blood and surrounding tissues[36]. In addition, properties, such as high biodegradability and minimal immune response and inflammatory response are required[37]. There is actively ongoing research and development of biomaterials with these characteristics that are capable of recovering or replacing damaged tissues in patients[38, 39]. Although various materials have been used for biomaterials, application of polymers has been investigated in several researches[40, 41]. Polymers are classified as natural or synthetic on the basis of their origin[42] (Figure 1-1). Synthetic polymers have the advantage to produce flexible materials with excellent mechanical properties[43].

Table 1-2. Characteristics of biomaterials.

	Synthetic Biomaterials	Natural biomaterials
Advantages	·Biocompatibility	·Biocompatibility ·Easily available ·Less toxicity ·Biodegradable
Disadvantages	·Non-degradable ·Toxicity ·Complicated synthetic process ·High cost	·Structurally more complex ·High degree of variability in natural materials derived from animal sources ·Complicated Extraction process

Among synthetic polymers, many medical materials capable of inducing regeneration and restoration of tissues in the human body have been studied[44]. Polyester polymers or copolymers are mainly used. These polymers are mostly chosen because of their high strength, ease of fabrication, corrosion resistance, low weight and low cost. However, synthetic polymers have lower mechanical strength than ceramic and metal materials and have lesser biocompatibility than natural polymers, which are highly biocompatible with naturally occurring polymeric materials[45, 46]. In general, biomaterials using natural polymers are biocompatible with cells and surrounding tissues, have excellent biodegradability, and are less inflammatory.

Among natural polymers, alginate has the advantages of absorbing body fluids and effectively maintaining moisture at wound sites[47]. In addition, alginate from seaweed is widely used in medical fields because of its biocompatibility, antibacterial activity, and biodegradation[48, 49].

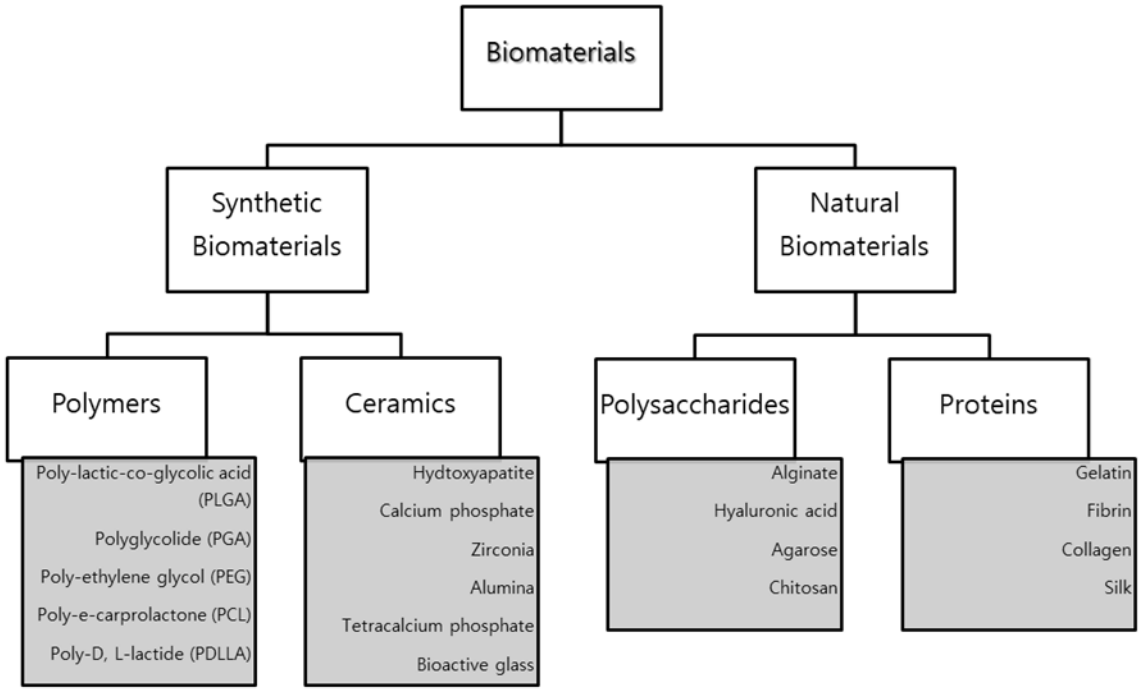

Figure 1-1. Classification of biomaterials.

1.3 Combinations of growth factors with biomaterials

Strategies for the application of growth factor with biomaterials have been studied in the last few years, with a particular focus on controlled release and bio-affinity growth factor immobilization[50].

1.3.1 Controlled release

One of the simplest methods to physically encapsulate a growth factor into a polymer matrix is to mix the growth factor with the polymers before their solidification or gelation. This strategy has the advantages that properties of scaffolds are not affected in the presence of factors and the bioactivity of growth factors can be maintained during their incorporation.

For example, Murphy et al. have improved VEGF encapsulated poly(lactic-co-glycolic acid) scaffold by introducing a growth factor[51]. Freeman et al. have synthesized sulfate–alginate/alginate scaffolds that include TGF-β1, platelet-derived growth factor, and VEGF. It was bound to sulfate–alginate with an affinity similar to that of heparin, thus enabling the delivery of three growth factors[52]. The results showed that vascularization within the triple growth factor-bound, alginate-based scaffolds was better than that found in scaffolds comprising a single growth factor following implantation in rats.

In addition, Hammond et al. prepared tetralayer structures using the layer by layer (LbL) strategy to capture and deliver growth factors by microgram scale, which resulted in incompletely stimulating host cell behaviors[53]. Another research used laponite clay as interlayer barriers in LbL films. It worked as a dual-purpose biomimetic microenvironment that gradually released the antibiotic. Then, BMP-2 was released for orthopedic implant applications[54]. These researches suggested that the LbL strategy could serve as a prospective delivery system for accurately controlled release of multiple drugs using component with different hydrolytic degradation rates.

1.3.2 Immobilization

Covalent immobilization of growth factors to biomaterials can greatly reduce the possibility of initial burst release. In addition, it has emerged as an approach for improving the persistence and stability of growth factors when delivered into a tissue or cell[55]. Covalent immobilization is preferred when the growth factor adsorbs by weak physisorption forces owing to inappropriate conformation or when the binding biomolecule is not able to adsorb on the surfaces. In contrast, covalently immobilized growth factors most commonly involve chemical reactions between functionalized surfaces and proteins, offering important control of the distribution, amount, and retention of growth factors in a solid matrix to facilitate growth factor delivery that is both sustained and localized. Carbodiimide coupling chemistry is one of the popular strategies for covalently grafting growth factors to various substrates because of its high conjugation ratio, simplicity, mild reaction conditions, and low cost[56].

As another immobilization approach, researchers have reported that mussels can strongly attach to various substrates because of 3,4-dihydroxy-L-phenylalanine (DOPA), which is the main active site for robust adhesion[57, 58]. Some research teams found that dopamine can be simply deposited on almost all types of organic and inorganic surfaces to form a polydopamine layer with a molecular structure similar to that of DOPA[59]. The advantages of polydopamine are robust adhesion properties to almost all types of substrates in mild conditions, regardless of the surface's chemical properties, and the formation of interlayers with high stability and affinity[60]. These researches using the reactivity of polydopamine to immobilize growth factors onto substrates provide a promising strategy for the sustained release of growth factors and effective loading, which finally improves implant integration and tissue repair.

In the other chemical coupling cases, several other types of reactive groups have also been studied to covalently attach growth factors to biocompatible substrates. For example, Leipzig et al. immobilized BMP-2 or PDGF-AA to photopolymerizable methacrylic chitosan through a streptavidin linker to induce neural cell differentiation *in vivo*[61]. Another research indicated the use of parylene coating in the immobilization of growth factors through a maleimide–thiol coupling reaction[62].

In extracellular matrix (ECM)-inspired growth factor delivery systems, a heparin-based binding approach from the natural interactions between growth factors and ECM has been devised for optimal delivery systems. The ECM is an immensely dynamic microenvironment that controls multiple cellular processes. Also, it acts as storage for growth factors because of the ability to bind molecules with high affinity. In particular, many growth factors, such as VEGF, BMP, and FGF, interact with the heparin sulfate of the ECM[63]. Consequently, many biomaterials have been used with heparin or heparin sulfate-like molecules, thus sequestering the heparin-binding ability of growth factors to enhance their delivery[64].

1.4 Insulin-like growth factor (IGF)

Insulin-like growth factor-1 (IGF-1) has received attention as a therapeutic factor for healing fractures. IGF-1, which is also known as somatomedin C, is a mitogenic factor that promotes not only adult cell growth but also embryo growth and differentiation[65, 66]. IGF-1 primarily comprises three helical structures corresponding to the two α-helices (IGF-1 residues 43–47 and 54–58) and a β-helix (IGF-1 residues 7–18) of insulin (Figure 1-2). The hydrophobic structure includes the following disulfide bonds: Cys 6–Cys 48, Cys 18–Cys 61, and Cys 47–Cys 52[67-69]. Residues 3–6 do not form any regular secondary structure[70]. As the electron density in residues 35–40 is weak and disconnected, this part has not been modeled. In the D-region, only

two residues—63 and 64—are arranged in the structure. IGF-1 and IGF-2 have different roles during the development of the human body. IGF-1 is an important growth hormone during childhood and adulthood, whereas IGF-2 primarily contributes during the fetal stage. It has been shown to improve the proliferation of stem cells and promotion of osteogenic differentiation[71]. Furthermore, poly (D,L-lactide) incorporated with TGF-β and IGF-1 can enhance fracture healing in rats without systemic adverse effects[72].

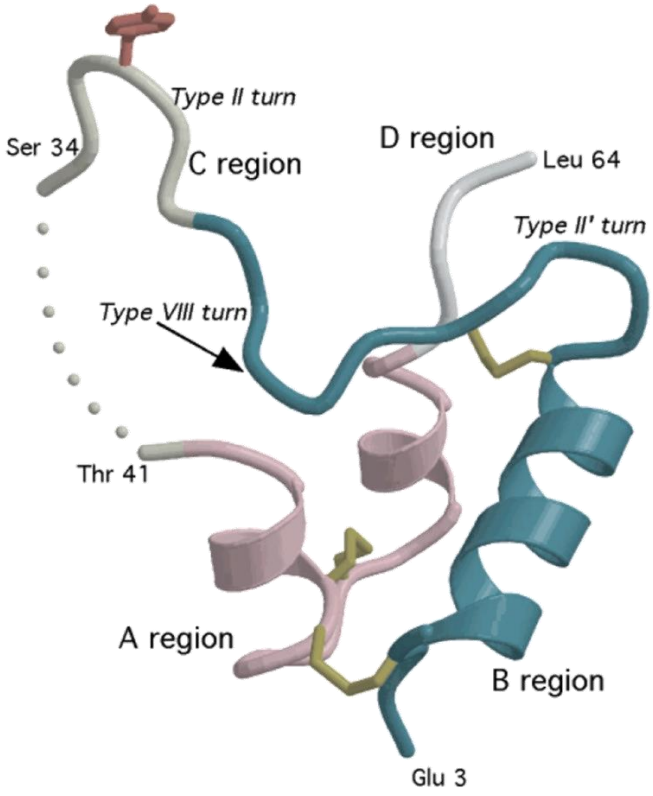

Figure 1-2. Structure of IGF-1 (ribbon structure). The B-region (residues 3–28) is shown in dark green, the C-region (residues 29–41) in dark gray, the A-region (residues 42–62) in purple, and the D-region (residues 63 and 64) in white. The three disulfides (Cys 6–Cys 48, Cys 18–Cys 61, and Cys 47–Cys 52) are shown in dark yellow.

1.5 Applications of IGF

IGF-1 has been applied in various ways to research on tissue regeneration, such as bone[73], cartilage[74], and nerve[75]. However, due to the various disadvantages of growth factors, biomaterials are required as carriers. There are many ways to utilize these biomaterials as carriers (Figure 1-3).

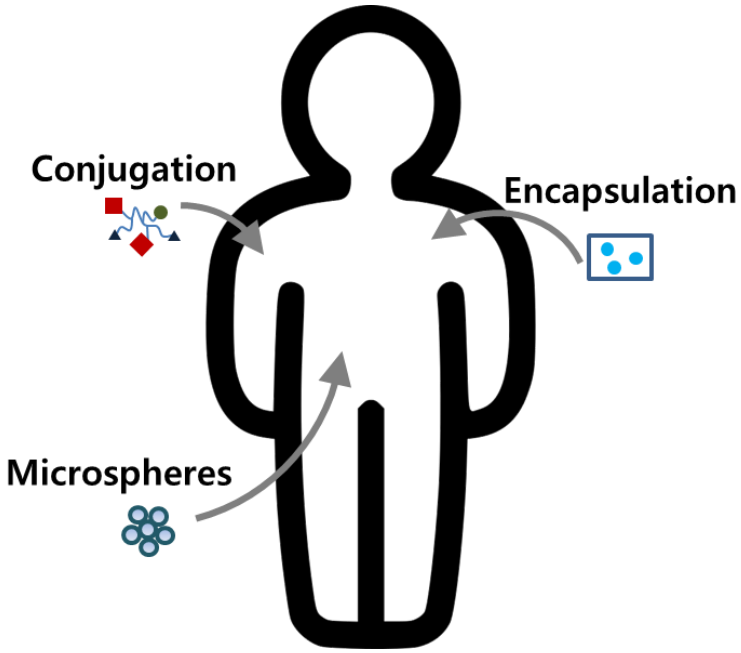

Figure 1-3. Application of IGF-1 using biomaterials.

First, there is a method of enclosing a growth factor in a biomaterial itself and delivering it[76]. Herein, one is a method of inserting a growth factor into a biomaterial after completing the form of the biomaterial[77]. In addition, there is another method of inserting a growth factor into a biomaterial before completion[78]. In the case of the former, the growth factor is diffused and released in a short time since it is sealed by a simple spread. However, the latter case is known to be easy to control the release of growth factors.

Second, there is a method of immobilizing a growth factor on the surface of a biomaterial[79]. The immobilized growth factor is not only involved in cell attachment but also regulates cell function by transferring cell signal.

Finally, the most widely used method is the growth factor delivery method using the micro-particle form of a biomaterial[80]. For preparing microparticles, the water-insoluble hydrophobic polymer material is dissolved using an organic solvent, the growth factor and emulsifier are added, and the organic solvent is evaporated to form micropores. In microspheres, the growth factor is released by diffusion and degradation of the polymer. At the beginning of the release, growth factors are mainly released by diffusion. To release the growth factor by the decomposition of the polymer, the structural stability of the protein should be considered. Through these methods, various biomaterials are actively used as carriers in research on tissue regeneration of growth factors.

1.6 This thesis

IGF-1 is essential for the maintenance, growth, and differentiation of cells. Accordingly, in the tissue regeneration study, the tissue regeneration effect of only IGF-1 itself was also studied in depth. Although the reported studies have shown efficacy, combination with appropriate biomaterials is expected to be more effective in tissue regeneration. Indeed, many studies have shown that the combination of IGF-1 and biomaterials is effective in tissue regeneration. Therefore, it is important to

understand the functions and characteristics of both IGF-1 and the biomaterial used and to combine them using the most appropriate method. Studies on the combination of IGF-1 and biomaterials should be continued to achieve the best effect in the regeneration of specific tissues. In this study, IGF-1 was encapsulated and released using photo-curable alginate. In addition, IGF-1 was conjugated with DOPA for improving initial cell growth and proliferation on titanium plate (Figure 1-4).

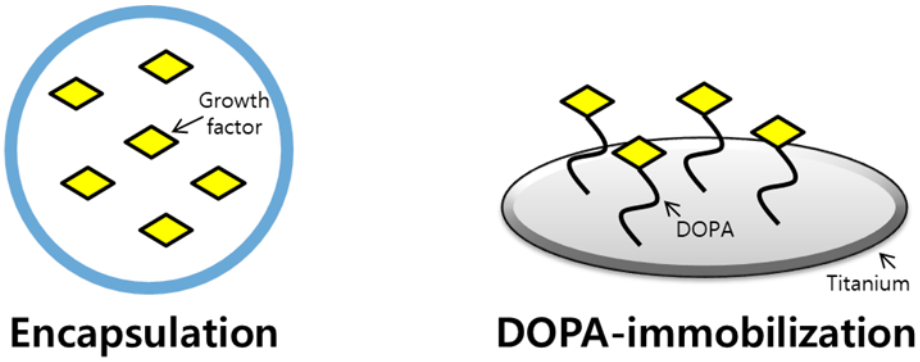

Figure 1-4. The strategies in this thesis.

1.7 References

1. K. Mukai, M. Tsai, H. Saito, S.J. Galli, Mast cells as sources of cytokines, chemokines, and growth factors, *Immunological Reviews*, 282, 121-150, 2018.

2. K. Bernard, N.J. Logsdon, G.A. Benavides, Y. Sanders, J. Zhang, V.M. Darley-Usmar, V.J. Thannickal, Glutaminolysis is required for transforming growth factor-β1–induced myofibroblast differentiation and activation, *Journal of Biological Chemistry*, 293, 1218-1228, 2018.

3. R. Cannarella, R. Condorelli, S.La. Vignera, A. Calogero, Effects of the insulin-like growth factor system on testicular differentiation and function: a review of the literature, *Andrology*, 6, 3-9, 2018.

4. C.S. Devignes, Y. Aslan, A. Brenot, A. Devillers, K. Schepers, S. Fabre, J. Chou, A.-J. Casbon, Z. Werb, S. Provot, HIF signaling in osteoblast-lineage cells promotes systemic breast cancer growth and metastasis in mice, *Proceedings of the National Academy of Sciences of the United States of America*, 115, E992-E1001, 2018.

5. Y. Xu, G.K.W. Kong, J.G. Menting, M.B. Margetts, C.A. Delaine, L.M. Jenkin, V.V. Kiselyov, P.De. Meyts, B.E. Forbes, M.C. Lawrence, How ligand binds to the type 1 insulin-like growth factor receptor, *Nature Communications*, 9, 821, 2018.

6. Q. Yao, Z. Yu, P. Liu, H. Zheng, Y. Xu, S. Sai, Y. Wu, C. Zheng, High Efficient Expression and Purification of Human Epidermal Growth Factor in Arachis Hypogaea L, *International Journal of Molecular Sciences*, 20, 2045, 2019.

7. M.R. Abbaszadegan, V. Bagheri, M.S. Razavi, A.A. Momtazi, A. Sahebkar, M. Gholamin, Isolation, identification, and characterization of cancer stem cells: A review, *Journal of Cellular Physiology*, 232, 2008-2018, 2017.

8. N. Ferrara, A.P. Adamis, Ten years of anti-vascular endothelial growth factor therapy, *Nature Reviews Drug Discovery*, 15, 385, 2016.

9. E.R. Castellanos, C. Ciferri, W. Phung, W. Sandoval, M.L. Matsumoto, Expression, purification, and characterization of recombinant human and murine milk fat globule-epidermal growth factor-factor 8, *Protein Expression and Purification*, 124, 10-22, 2016.

10. T.A. Wynn, K.M. Vannella, Macrophages in tissue repair, regeneration, and fibrosis, *Immunity*, 44, 450-462, 2016.

11. S. Gnavi, L.di. Blasio, C. Tonda-Turo, A. Mancardi, L. Primo, G. Ciardelli, G. Gambarotta, S. Geuna, I. Perroteau, Gelatin-based hydrogel for vascular endothelial growth factor release in peripheral nerve tissue engineering, *Journal of Tissue Engineering and Regenerative Medicine*, 11, 459-470, 2017.

12. V. David, A. Martin, T. Isakova, C. Spaulding, L. Qi, V. Ramirez, K.B. Zumbrennen-Bullough, C.C. Sun, H.Y. Lin, J.L. Babitt, Inflammation and functional iron deficiency regulate fibroblast growth factor 23 production, *Kidney International*, 89, 135-146, 2016.

13. J. Tabernero, R. Bahleda, R. Dienstmann, J.R. Infante, A. Mita, A. Italiano, E. Calvo, V. Moreno, B. Adamo, A. Gazzah, Phase I dose-escalation study of JNJ-42756493, an oral pan–fibroblast growth factor receptor inhibitor, in patients with advanced solid tumors, *Journal of Clinical Oncology*, 33, 3401-3408, 2015.

14. Y. Enuka, M. Lauriola, M.E. Feldman, A. Sas-Chen, I. Ulitsky, Y. Yarden, Circular RNAs are long-lived and display only minimal early alterations in response to a growth factor, *Nucleic Acids Research*, 44, 1370-1383, 2015.

15. K. Takeda, H. Kitagawa, R. Tsuboi, W. Kiba, J.I. Sasaki, M. Hayashi, S. Imazato, Effectiveness of non-biodegradable poly (2-hydroxyethyl methacrylate)-based

hydrogel particles as a fibroblast growth factor-2 releasing carrier, *Dental Materials*, 31, 1406-1414, 2015.

16. J. Li, D.J. Mooney, Designing hydrogels for controlled drug delivery, *Nature Reviews Materials*, 1, 16071, 2016.

17. M. Datta, L.E. Via, W.S. Kamoun, C. Liu, W. Chen, G. Seano, D.M. Weiner, D. Schimel, K. England, J.D. Martin, Anti-vascular endothelial growth factor treatment normalizes tuberculosis granuloma vasculature and improves small molecule delivery, *Proceedings of the National Academy of Sciences of the United States of America*, 112, 1827-1832, 2015.

18. P. Vader, E.A. Mol, G. Pasterkamp, R.M. Schiffelers, Extracellular vesicles for drug delivery, *Advanced Drug Delivery Reviews*, 106, 148-156, 2016.

19. E. Migliorini, A. Valat, C. Picart, E.A. Cavalcanti-Adam, Tuning cellular responses to BMP-2 with material surfaces, *Cytokine & Growth Factor Reviews*, 27, 43-54, 2016.

20. M.A. Eskander, S. Ruparel, D.P. Green, P.B. Chen, E.D. Por, N.A. Jeske, X. Gao, E.R. Flores, K.M. Hargreaves, Persistent nociception triggered by nerve growth factor (NGF) is mediated by TRPV1 and oxidative mechanisms, *Journal of Neuroscience*, 35, 8593-8603, 2015.

21. A. Grabner, A.P. Amaral, K. Schramm, S. Singh, A. Sloan, C. Yanucil, J. Li, L.A. Shehadeh, J.M. Hare, V. David, Activation of cardiac fibroblast growth factor receptor 4 causes left ventricular hypertrophy, *Cell Metabolism*, 22, 1020-1032, 2015.

22. S.K. Denduluri, O. Idowu, Z. Wang, Z. Liao, Z. Yan, M.K. Mohammed, J. Ye, Q. Wei, J. Wang, L. Zhao, Insulin-like growth factor (IGF) signaling in tumorigenesis and the development of cancer drug resistance, *Genes and Diseases*, 2, 13-25, 2015.

23. R. Roskoski Jr, Vascular endothelial growth factor (VEGF) and VEGF receptor inhibitors in the treatment of renal cell carcinomas, *Pharmacological Research*, 120, 116-132, 2017.

24. M. Hara-Chikuma, S. Watanabe, H. Satooka, Involvement of aquaporin-3 in epidermal growth factor receptor signaling via hydrogen peroxide transport in cancer cells, *Biochemical and Biophysical Research Communications*, 471, 603-609, 2016.

25. Z. Luo, L. Jiang, Y. Xu, H. Li, W. Xu, S. Wu, Y. Wang, Z. Tang, Y. Lv, L. Yang, Mechano growth factor (MGF) and transforming growth factor (TGF)-β3 functionalized silk scaffolds enhance articular hyaline cartilage regeneration in rabbit model, *Biomaterials*, 52, 463-475, 2015.

26. N. Huebsch, D.J. Mooney, Inspiration and application in the evolution of biomaterials, *Nature*, 462, 426, 2009.

27. A.E. Engberg, P.H. Nilsson, S. Huang, K. Fromell, O.A. Hamad, T.E. Mollnes, J.P. Rosengren-Holmberg, K. Sandholm, Y. Teramura, I.A. Nicholls, Prediction of inflammatory responses induced by biomaterials in contact with human blood using protein fingerprint from plasma, *Biomaterials*, 36, 55-65, 2015.

28. W.J. Li, R. Tuli, C. Okafor, A. Derfoul, K.G. Danielson, D.J. Hall, R.S. Tuan, A three-dimensional nanofibrous scaffold for cartilage tissue engineering using human mesenchymal stem cells, *Biomaterials*, 26, 599-609, 2005.

29. P. Zartner, R. Cesnjevar, H. Singer, M. Weyand, First successful implantation of a biodegradable metal stent into the left pulmonary artery of a preterm baby, *Catheterization and Cardiovascular Interventions*, 66, 590-594, 2005.

30. L.B. Enda, S. Rose, K. Nicola, A.S. Caoimhe, E.M. Peter, A review of material degradation modelling for the analysis and design of bioabsorbable stents, *Annals of Biomedical Engineering*, 44, 341-356, 2016.

31. G.G. Stefanini, R.A. Byme, P.W. Serruys, A. de Waha, B. Meier, S. Massberg, P. Juni, A. Schomig, S. Windecker, A. Kastrati, Biodegradable polymer drug-eluting stents reduce the risk of stent thrombosis at 4 years in patients undergoing percutaneous coronary intervention, *European Heart Journal*, 10, 1214-1222, 2012.

32. S.S.D. Kumar, N.K. Rajendran, N.N. Houreld, H. Abrahamse, Recent advances on silver nanoparticle and biopolymer-based biomaterials for wound healing applications, *International Journal of Biological Macromolecules*, 115, 165-175, 2018.

33. A.J. Teo, A. Mishra, I. Park, Y.J. Kim, W.T. Park, Y.J. Yoon, Polymeric biomaterials for medical implants and devices, *ACS Biomaterials Science & Engineering*, 2, 454-472, 2016.

34. D. Sun, M.B. Shahzad, M. Li, G. Wang, D. Xu, Antimicrobial materials with medical applications, *Materials Technology*, 30, B90-B95, 2015.

35. F. Khan, M. Tanaka, S.R. Ahmad, Fabrication of polymeric biomaterials: a strategy for tissue engineering and medical devices, *Journal of Materials Chemistry B*, 3, 8224-8249, 2015.

36. Y. Ramot, M. Haim-Zada, A.J. Domb, A. Nyska, Biocompatibility and safety of PLA and its copolymers, *Advanced Drug Delivery Reviews*, 107, 153-162, 2016.

37. A. Vishwakarma, N.S. Bhise, M.B. Evangelista, J. Rouwkema, M.R. Dokmeci, A.M. Ghaemmaghami, N.E. Vrana, A. Khademhosseini, Engineering

immunomodulatory biomaterials to tune the inflammatory response, *Trends in Biotechnology*, 34, 470-482, 2016.

38. M.E. Ogle, C.E. Segar, S. Sridhar, E.A. Botchwey, Monocytes and macrophages in tissue repair: Implications for immunoregenerative biomaterial design, *Experimental Biology and Medicine*, 241, 1084-1097, 2016.

39. T.H. Qazi, D.J. Mooney, M. Pumberger, S. Geissler, G.N. Duda, Biomaterials based strategies for skeletal muscle tissue engineering: existing technologies and future trends, *Biomaterials*, 53, 502-521, 2015.

40. S. Affatato, A. Ruggiero, M. Merola, Advanced biomaterials in hip joint arthroplasty. A review on polymer and ceramics composites as alternative bearings, *Composites Part B: Engineering*, 83, 276-283, 2015.

41. Z. Shi, X. Gao, M.W. Ullah, S. Li, Q. Wang, G. Yang, Electroconductive natural polymer-based hydrogels, *Biomaterials*, 111, 40-54, 2016.

42. M. Sohail, M.U. Minhas, S. Khan, Z. Hussain, M. de Matas, S.A. Shah, S. Khan, M. Kousar, K. Ullah, Natural and synthetic polymer-based smart biomaterials for management of ulcerative colitis: A review of recent developments and future prospects, *Drug Delivery and Translational Research*, 9, 595-614, 2019.

43. D.P. Yang, Z. Li, M. Liu, X. Zhang, Y. Chen, H. Xue, E. Ye, R. Luque, Biomass-derived carbonaceous materials: recent progress in synthetic approaches, advantages and applications, *ACS Sustainable Chemistry & Engineering*, 7, 4564-4585, 2019.

44. W.L. Brooks, B.S. Sumerlin, Synthesis and applications of boronic acid-containing polymers: from materials to medicine, *Chemical reviews*, 116, 1375-1397, 2015.

45. M.C. Demirel, M. Cetinkaya, A. Pena-Francesch, H. Jung, Recent advances in nanoscale bioinspired materials, *Macromolecular Bioscience*, 15, 300-311, 2015.

46. S. Singh, S. Ramakrishna, R. Singh, Material issues in additive manufacturing: a review, *Journal of Manufacturing Processes*, 25, 185-200, 2017.

47. E. Ruvinov, S. Cohen, Alginate biomaterial for the treatment of myocardial infarction: progress, translational strategies, and clinical outlook: from ocean algae to patient bedside, *Advanced Drug Delivery Reviews*, 96, 54-76, 2016.

48. N. Lin, A. Gèze, D. Wouessidjewe, J. Huang, A. Dufresne, Biocompatible double-membrane hydrogels from cationic cellulose nanocrystals and anionic alginate as complexing drugs codelivery, *ACS Applied Materials & Interfaces*, 8, 6880-6889, 2016.

49. H. Chen, X. Xing, H. Tan, Y. Jia, T. Zhou, Y. Chen, Z. Ling, X. Hu, Covalently antibacterial alginate-chitosan hydrogel dressing integrated gelatin microspheres containing tetracycline hydrochloride for wound healing, *Materials Science and Engineering: C*, 70, 287-295, 2017.

50. F. Chen, Y. An, R. Zhang, M. Zhang, New insights into and novel applications of release technology for periodontal reconstructive therapies, *Journal of Controlled Release*, 149, 92-110, 2011.

51. W.L. Murphy, M.C. Peters, D.H. Kohn, D.J. Mooney, Sustained release of vascular endothelial growth factor from mineralized poly(lactide-co-glycolide) scaffolds for tissue engineering, *Biomaterials*, 21, 2521-2527, 2000.

52. I. Freeman, S. Cohen, The influence of the sequential delivery of angiogenic factors from affinity-binding alginate scaffolds on vascularization, *Biomaterials*, 30, 2122-2131, 2009.

53. M.L. Macdonald, R.E. Samuel, N.J. Shah, R.F. Padera, Y.M. Beben, P.T. Hammomd, Tissue integration of growth factor-eluting layer-by-layer polyelectrolyte multilayer coated implants, *Biomaterials*, 32, 1446-1453, 2011.

54. J. Min, R.D. Braatz, P.T. Hammond, Tunable staged release of therapeutics from layer-by-layer coatings with clay interlayer barrier, *Biomaterials*, 35, 2507-2517, 2014.

55. K.S. Masters, Covalent growth factor immobilization strategies for tissue repair and regeneration, *Macromolecular Bioscience*, 11, 1149-1163, 2011.

56. L. Liu, Y. Xing, S. Li, B. Yuan, J. Chen, N. Xia, Activity analysis of the carbodiimide-mediated amine coupling reaction on self-assembled monolayers by cyclic voltammetry, *Electrochimica Acta*, 89, 616-622, 2013.

57. J.H. Waite, X. Qin, Polyphosphoprotein from the adhesive pads of Mytilus edulis, *Biochemistry*, 40, 2887-2893, 2001.

58. M.J. Harrington, A. Masic, N. Holten-Andersen, J.H. Waite, P. Fratzl, Iron-clad fibers: a metal-based biological strategy for hard flexible coatings, *Science*, 328, 216-220, 2010.

59. H. Lee, S.M. Dellatore, W.M. Miller, P.B. Messersmith, Mussel-inspired surface chemistry for multifunctional coatings, *Science*, 318, 426-430, 2007.

60. Y. Liu, K. Ai, L. Lu, Polydopamine and its derivative materials: synthesis and promising applications in energy, environmental, and biomedical fields, *Chemical Reviews*, 114, 5057-5115, 2014.

61. H. Li, A.M. Koenig, P. Sloan, N.D. Leipzig, In vivo assessment of guided neural stem cell differentiation in growth factor immobilized chitosan-based hydrogel scaffolds, *Biomaterials*, 35, 9049-9057, 2014.

62. Y.C. Chen, T.P. Sun, C.T. Su, J.T. Wu, C.Y. Lin, J. Yu, C.W. Huang, Sustained immobilization of growth factor proteins based on functionalized parylenes, *ACS Applied Materials & Interfaces*, 6, 21906-21910, 2014.

63. I. Capila, R.J. Linhardt, Heparin-protein interactions, *Angewandte Chemie International Edition*, 41, 390-412, 2002.

64. A.K. Jha, A. Mathur, F.L. Svedlund, J. Ye, Y. Yeghiazarians, K.E. Healy, Molecular weight and concentration of heparin in hyaluronic acid-based matrices modulates growth factor retention kinetics and stem cell fate, *Journal of Controlled Release*, 209, 308-316, 2015.

65. E. Sanchez-Lopez, E. Flashner-Abramson, S. Shalapour, Z. Zhong, K. Taniguchi, A. Levitzki, M. Karin, Targeting colorectal cancer via its microenvironment by inhibiting IGF-1 receptor-insulin receptor substrate and STAT3 signaling, *Oncogene*, 35, 2634, 2016.

66. J. Yan, J.W. Herzog, K. Tsang, C.A. Brennan, M.A. Bower, W.S. Garrett, B.R. Sartor, A.O. Aliprantis, J.F. Charles, Gut microbiota induce IGF-1 and promote bone formation and growth, *Proceedings of the National Academy of Sciences of the United States of America*, 113, E7554-E7563, 2016.

67. R. M. Cooke, T. S. Harvey, I. D. Campbell, Solution structure of human insulin-like growth factor 1: a nuclear magnetic resonance and restrained molecular dynamics study, *Biochemistry, 30*, 5484-5491, 1991.

68. E. de Wolf, R. Gill, S. Geddes, J. Pitts, A. Wollmer, J. Grotzinger, Solution structure of a mini IGF-1, *Protein Science, 5*, 2193-2202, 1996.

69. L. G. Laajoki, G. L. Francis, J. C. Wallace, J. A. Carver, M. A. Keniry, Solution structure and backbone dynamics of long-[Arg3] insulin-like growth factor-I, *Journal of Biological Chemistry, 275*, 10009-10015, 2000.

70. U. Derewenda, Z. Derewenda, E.J. Dodson, G.G. Dodson, C.D. Reynolds, G.D. Smith, C. Sparks, D. Swenson, Phenol stabilizes more helix in a new symmetrical zinc insulin hexamer, *Nature*, *338*, 594-596, 1989.

71. M. Yu, H. Wang, Y. Xu, D. Yu, D. Li, X. Liu, W. Du, Insulin-like growth factor-1 (IGF-1) promotes myoblast proliferation and skeletal muscle growth of embryonic chickens via the PI3K/Akt signalling pathway, *Cell Biology International*, 39, 910-922, 2015.

72. T. Gao, N. Zhang, Z. Wang, Y. Wang, Y. Liu, Y. Ito, P. Zhang, Biodegradable microcarriers of poly (lactide-co-glycolide) and nano-hydroxyapatite decorated with IGF-1 via polydopamine coating for enhancing cell proliferation and osteogenic differentiation, *Macromolecular Bioscience*, 15, 1070-1080, 2015.

73. D.D. Bikle, C. Tahimic, W. Chang, Y. Wang, A. Philippou, E.R. Barton, Role of IGF-I signaling in muscle bone interactions, *Bone*, 80, 79-88, 2015.

74. D.J. Griffin, K.F. Ortved, A.J. Nixon, L.J. Bonassar, Mechanical properties and structure–function relationships in articular cartilage repaired using IGF-I gene-enhanced chondrocytes, *Journal of Orthopaedic Research*, 34, 149-153, 2016.

75. S.H. Tuffaha, J.D. Budihardjo, K.A. Sarhane, M. Khusheim, D. Song, J.M. Broyles, R. Salvatori, K.R. Means, J.P. Higgins, J.T. Shores, Growth hormone therapy accelerates axonal regeneration, promotes motor reinnervation, and reduces muscle atrophy following peripheral nerve injury, *Plastic and Reconstructive Surgery*, 137, 1771-1780, 2016.

76. R.J. Smith Jr, M.T. Koobatian, A. Shahini, D.D. Swartz, S.T. Andreadis, Capture of endothelial cells under flow using immobilized vascular endothelial growth factor, *Biomaterials*, 51, 303-312, 2015.

77. A. Sculean, D. Nikolidakis, G. Nikou, A. Ivanovic, I.L. Chapple, A. Stavropoulos, Biomaterials for promoting periodontal regeneration in human intrabony defects: a systematic review, *Periodontology*, *2000*, 68, 182-216, 2015.

78. F. Anjum, P.S. Lienemann, S. Metzger, J. Biernaskie, M.S. Kallos, M. Ehrbar, Enzyme responsive GAG-based natural-synthetic hybrid hydrogel for tunable growth factor delivery and stem cell differentiation, *Biomaterials*, 87, 104-117, 2016.

79. Z. Wang, L. Chen, Y. Wang, X. Chen, P. Zhang, Improved cell adhesion and osteogenesis of op-HA/PLGA composite by poly (dopamine)-assisted immobilization of collagen mimetic peptide and osteogenic growth peptide, *ACS Applied Materials & Interfaces*, 8, 26559-26569, 2016.

80. E. Quinlan, A. López-Noriega, E.M. Thompson, A. Hibbitts, S.A. Cryan, F.J. O'Brien, Controlled release of vascular endothelial growth factor from spray-dried alginate microparticles in collagen-hydroxyapatite scaffolds for promoting vascularization and bone repair, *Journal of Tissue Engineering and Regenerative Medicine*, 11, 1097-1109, 2017.

CHAPTER 2

CONTROLLED RELEASE OF IGF

2.1 Introduction

Photochemistry plays an important role in medical applications including diagnosis and therapy[1]. Many types of photo-reactive material have been developed for medical applications[1]. The most common application is as a dental material[1-5]. Some light-curable resins have been developed with the development of photo-initiators. The photo-reactive mechanism of dental resins is mainly based on polymerization by photo-initiators which produce a free radical during photo-irradiation. In addition to these dental resins, photo-initiator-based quasi-living polymerization[6], polymerization using visible or UV-light initiators[7-10], type 2 photo-initiation using silk peptides[11] or photo-initiation polymerization by riboflavin (vitamin B-2)[12-15] have been investigated for biomaterials.

For soft and hard tissue applications, and tissue interfaces, photo-reactive polymers based on photo- crosslinking mechanisms have been developed. They are classified for surface treatment[16-24] and bulk gelation[25-28]. Widely used UV-reactive functional groups include azidophenyl[16-22, 28], benzophenone[23], diazirine[24] and cycloaddition forming reaction[25-27]. However, the direct use of UV light in the body has risks, including cancer, immune impairment, and genetic mutations[29- 31].

Therefore, in recent years, visible-light-reactive natural polymers have been developed[1, 2, 32]. This includes natural polymers conjugated with furan, which is easily oxidized by visible light-irradiation in the presence of photo sensitizers. As natural polymers, DNA[33], gelatin[34-36], chitosan[37, 38], alginate[39, 40] and hyaluronic acid[41] have been employed. From oxygen molecules the photosensitizer generates singlet oxygen which reacts with the furan derivative to offer photo- crosslinking via furan endoperoxide formation caused by the irradiation[34, 42, 43]. Furan-natural polymer conjugates have been used for tissue engineering[44, 45].

Insulin-like growth factor-1 (IGF-1), which promotes not only adult cell growth but also embryonic growth and differentiation, has received attention as a therapeutic factor for fracture healing[46]. It has been shown to improve the proliferation of stem cells and reverse the inhibition of osteogenic differentiation by implants[47, 48].

Previously, we prepared a furan-alginate conjugate for visible light-curable gel formation in the presence of Rose Bengal[39, 40]. However, previous studies investigated only one composition of furfuryl alginate. In the current study, the chemical bond formation of an alginate-conjugated furan was confirmed through Fourier transform infrared spectroscopy (FT-IR) and two types of photosensitizer were employed. In addition, through adjustment of the preparation pH, the incorporation of various furan groups into the alginate was enabled. Therefore, composition-dependent hydrogel formation was quantitatively investigated using a rheometer. Importantly, some properties of the visible light-curable gel were compared with those of an alginate gel with conventional Ca^{2+}-induced gelation.

2.2 Materials and methods

2.2.1 Materials

Sodium alginate (viscosity of 1000 centipoise), hydrochloric acid, benzyl alcohol, Rose Bengal and riboflavin were purchased from Wako Pure Chemical (Osaka, Japan). Furfurylamine (Sigma-Aldrich, St. Louis, MO, USA), 1-ethyl-3-(3-dimethylaminopropyl) carbodiimide hydrochloride (EDC, Tokyo Chemical Industry, Tokyo Japan), N-hydroxysuccinimide (NHS, Tokyo Chemical Industry), and fluorescein isothiocyanate (FITC, Sigma-Aldrich) were used as received. Dextran with a molecular weight of 4000, 10000, or 70000 labeled with FITC, Alexa Fluor 488, or Oregon Green 488 was purchased from Sigma-Aldrich, and Thermo Fisher

Scientific (Waltham, MA, USA), and this was referred to as Dex4k, Dex10k, and Dex70k, respectively. FITC-conjugated bovine albumin (BSA) and insulin-like growth factor-1 (IGF-1) were purchased from Sigma-Aldrich and R&D Systems (Minneapolis, MN, USA), respectively.

2.2.2 Preparation of photo-curable alginate

Furfuryl alginate was prepared in accordance with a previously reported method[39] (Figure 2-1). Briefly, 200 mg of sodium alginate was dissolved in 20 mL of 2-(N-morpholino) ethanesulfonic acid buffer for pH adjustment at room temperature. Subsequently, EDC (150 mg) and NHS (100 mg) were added and stirred for 30 min. After all the compounds had dissolved, furfurylamine was added dropwise and the solution was stirred at 60℃ for 20 h. The pH was adjusted to 7.0 using a diluted hydrochloric acid solution and dialyzed against Milli-Q water using a dialysis membrane (MWCO: 10000, Spectra/Por 6, Spectrum Laboratories, Rancho Dominguez, CA) for 5 days at room temperature to completely remove all of the unreacted reactants and the byproducts. The dialyzed samples were lyophilized to obtain a white powder. The modified alginate is referred to as F-Alginate.

^{1}H NMR spectra were recorded using an ECZ-400 spectrometer (400 MHz, JEOL, Tokyo, Japan). D_2O was used for ^{1}H NMR measurement without any internal standard. To determine the content of furfuryl units in F-Alginate, 2 mg/mL of benzyl alcohol (as an internal reference) was added to the F-Alginate solution (10 mg/mL). The infrared (IR) absorbance of furfurylamine, sodium alginate and F-Alginate was analyzed using a Fourier transform infrared spectrometer (FT-IR 4100, JASCO, Tokyo,

Japan). All samples were dissolved in PBS (pH 7.4) and solution samples (3 mg/mL) were measured by the attenuated total reflection (ATR) mode using the prism of zinc selenide.

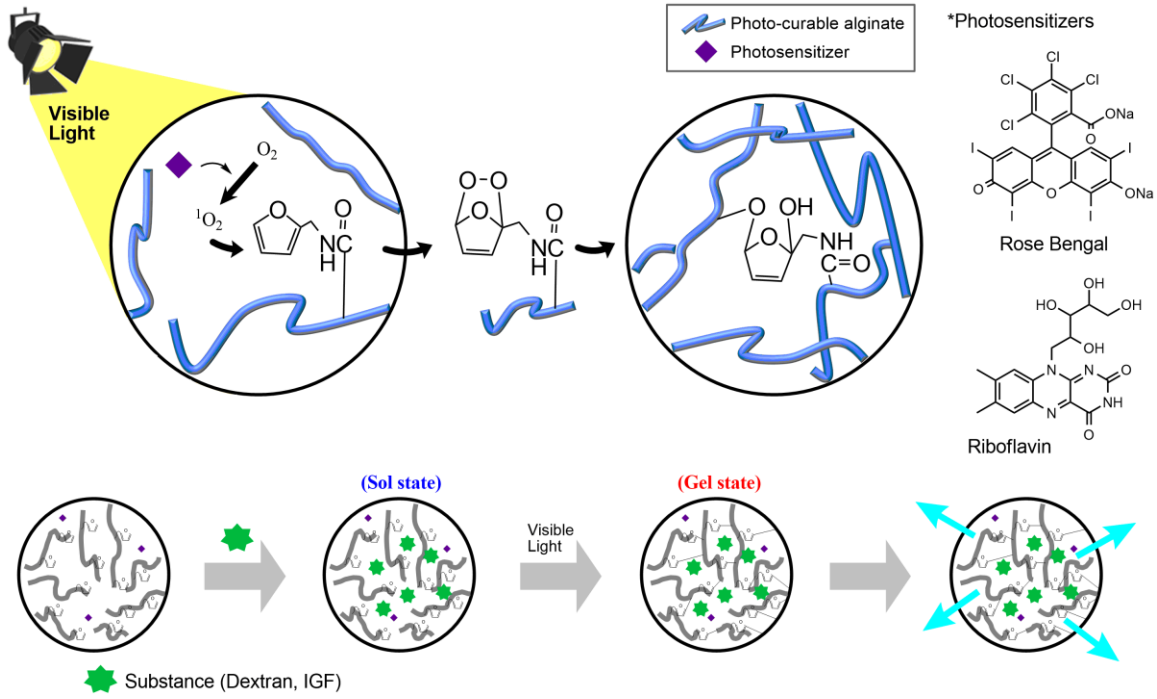

Figure 2-1. Diagram of the photo-crosslinking of photo-curable alginate (F-Alginate) containing a photosensitizer through visible light exposure and encapsulation of substance.

2.2.3 Photo-curing of F-Alginate

F-Alginate solutions (concentration: 1, 3, 5, and 10%) were mixed with a photosensitizer (Rose Bengal or riboflavin). The mixtures were cast on a 24-well polystyrene plate (Iwaki, Tokyo, Japan) and were irradiated with visible light at a distance of 1 cm for 1–10 min at 40℃ using an LED light source (LA-HDF158A, Hayashi Watch Works, Tokyo, Japan). The light intensity at 445 and 548 nm was 200 and 100 mW, respectively. Subsequently, the resultant product was rinsed with 1 mL of Dulbecco's modified phosphate-buffered saline (PBS) for 10 min on a shaker (300 rpm) at room temperature and the weight of the dried gel was measured before and after the visible light exposure.

As a control sample, Ca^{2+}-crosslinked alginate (C-Alginate) was prepared by mixing a 10% aqueous solution of sodium alginate with aqueous solutions of different $CaCl_2$ concentrations at room temperature.

2.2.4 Viscoelasticity measurement

The viscosity and mechanical properties were recorded using an AR G2 rheometer (TA Instruments, New Castle, DE, USA). F-Alginate (10%) was mixed with the photosensitizer (0.2%) and 200 μL of mixture was casted on the plate. Visible light was exposed to the sample for 10 min at 40°C. Elastic modulus (G') and loss modulus (G'') were recorded using the rheometer at a frequency of 1 Hz and a strain of 1%.

2.2.5 Incorporation of molecules and release profile

An F-Alginate (1:1) solution was mixed with 100 nM of fluorescein, IGF-1, Dex4k, Dex10k, Dex70k or BSA, and the mixtures were cast on a 24-well plate. After the samples were exposed to visible light for 10 min at 40℃, they were rinsed with PBS once, followed by incubation in 1 mL of PBS at room temperature. At predetermined periods, the supernatant was recovered and the fluorescence intensity was recorded using an FP-6500 spectrofluorometer (JASCO) ($\lambda_{excitation}$: 495 nm and $\lambda_{emission}$: 520 nm).

The amount of IGF-1 was determined using an enzyme linked immunosorbent assay (ELISA) kit (ab211651, Abcam, Cambridge, UK). The analyte solution (50 µL) and antibody cocktail solutions were mixed in a 96-well ELISA plate. The plate was incubated for 1 h at room temperature on a plate shaker (400 rpm). After removal of the solution, each well was washed three times using 200 µL of the washing buffer. A tetramethylbenzidine solution (100 µL) was added to each well and incubated for 10 min on a plate shaker (400 rpm) under dark conditions. The stop solution (100 µL) was added to each well and the plate was stirred on the shaker for 1 min. Finally, the absorbance (450 nm) of the solution was measured using a microplate reader (EnSpire Alpha 2390; Perkin-Elmer, Waltham, MA, USA).

2.2.6 Cell culture

Mouse fibroblast NIH/3T3 (3T3) cells were provided by the RIKEN Cell Bank (Tsukuba, Japan) and were cultured in Dulbecco's modified Eagle medium (Sigma-Aldrich) with 10% fetal bovine serum (FBS) at 37℃ in a humidified atmosphere containing 5% CO_2 and 95% air. Cells were harvested using a 1 mM ethylenediaminetetraacetic acid and 0.25% trypsin solution (Sigma-Aldrich). Trypan blue solution (0.5%, Nacalai Tesque, Kyoto, Japan) was used to stain live cells prior to

live cell counting. For the live/dead and proliferation assay, 2×10^4 cells/mL and 1×10^4 cells/mL were seeded per well, respectively. The culture medium was exchanged at 12 h. The solid samples were washed twice using 500 μL of PBS before the cell experiments.

2.2.7 Cell assay

The cell counting was performed using a Cell Counting Kit-8 (Dojindo, Kumamoto, Japan) in accordance with the manufacturer's instructions. The absorbance at 450 nm was measured using a microplate reader.

The cell viability was investigated using a LIVE/DEAD viability/cytotoxicity kit (Thermo Fisher Scientific). The cells were washed using PBS and exposed to ethidium homodimer-1 (4 μM) and calcein AM (2 μM) solutions at room temperature for 30 min. Fluorescent images were obtained using a fluorescence microscope (Olympus, Tokyo, Japan).

2.2.8 Statistical analysis

Statistical analysis was performed using Excel software (Microsoft, WA, USA). An analysis of variance was performed to compare a single group at multiple time points or multiple groups at one time point. If the F ratio was significant either for an interaction or for a main effect between the effect and time, then the differences were specified using Student's t-test. A two-way paired t-test was performed to compare one group over two time points, and the two-way unpaired t-test was performed to compare two groups at a single time point. Data are shown as mean ± SEM. $p<0.05$ was interpreted as statistically significant.

2.3 Results and discussion

2.3.1 Characterization of F-Alginate

The viscosity was measured using a rheometer as shown in Figure 2-2. $[\eta]_0$ of sodium alginate was calculated to be 11.4. The molecular weight of sodium alginate was determined from the Mark–Houwink–Sakurada equation[49],

$$[\eta] = KM^a$$

where, $[\eta]$ is an intrinsic viscosity in 1 N NaCl solution at 25℃, M is the molecular weight of sodium alginate, and K and a is 0.362×10^{-3} and 1.2, respectively[50]. It was calculated as 1,110,000.

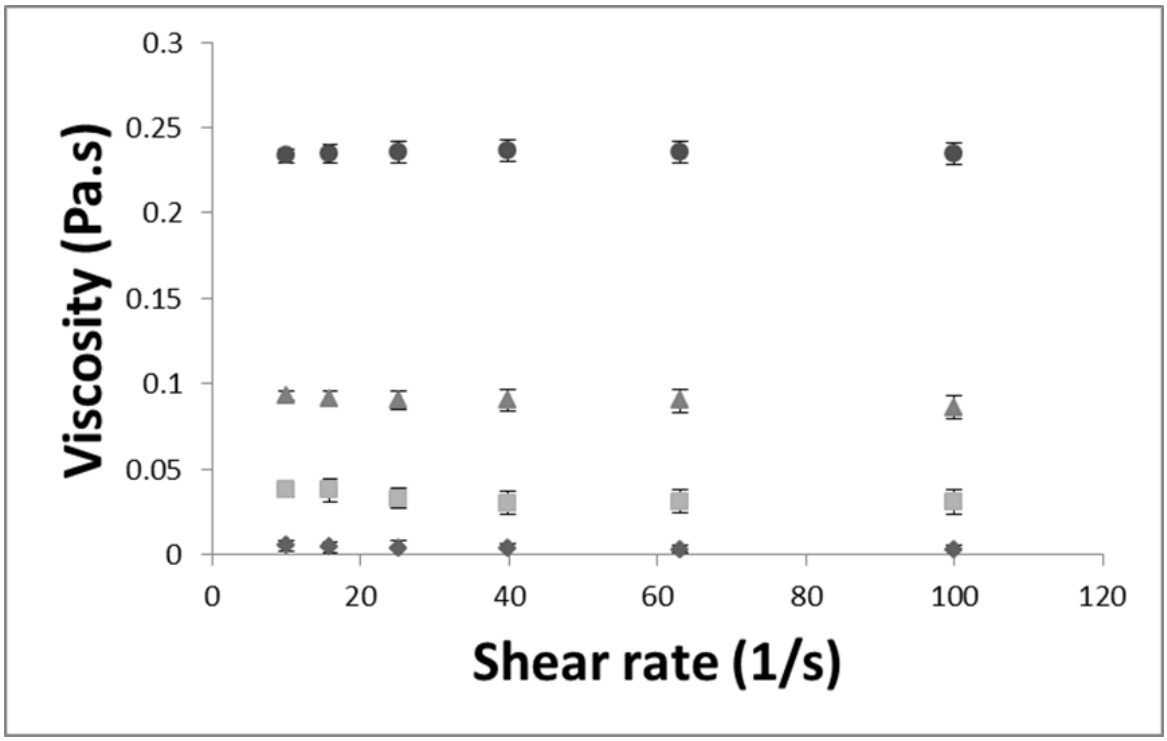

Figure 2-2. The viscosity of sodium alginate. The concentration of sodium alginate was 1.25 mg/mL (◆), 2.5 mg/mL (■), 5 mg/mL (▲) and 10 mg/mL (●). n=3.

The FT-IR spectra of alginate, furfurylamine, and F-Alginate are shown in Figure 2-3. The IR spectrum of alginate exhibited a C=O stretching vibration of the carboxyl group in the α-D-mannuronic acid and β-L-guluronic acid as a peak at 1725 cm^{-1}. After conjugation with furfurylamine, the IR spectrum of F-Alginate showed a C=O peak at 1670 cm^{-1} corresponding to the formed amide group in addition to the peaks observed in unmodified alginate. The IR results indicate that the furfuryl group had been successfully introduced into the alginate.

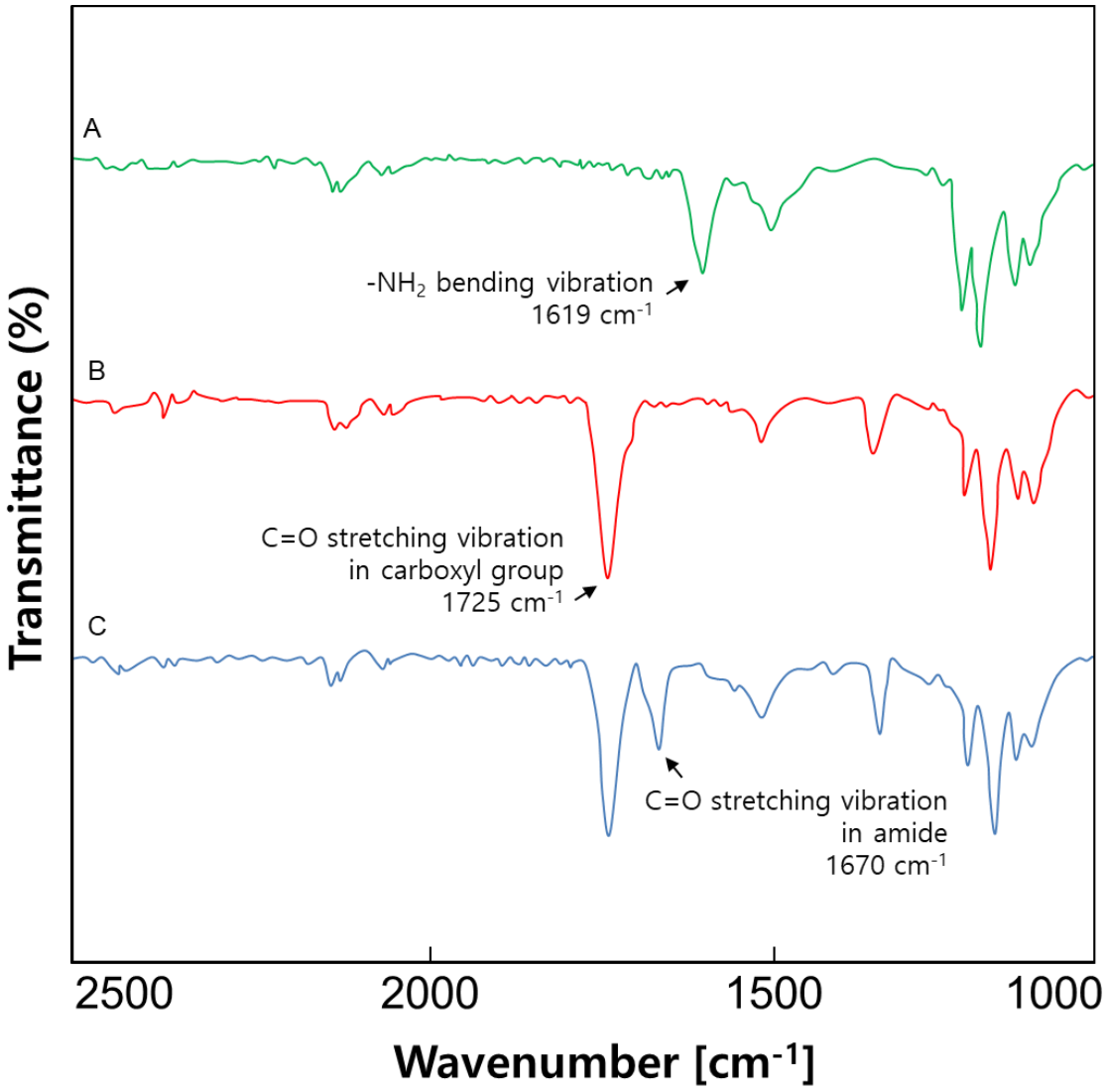

Figure 2-3. Fourier transform infrared spectra of furfurylamine (A), sodium alginate (B) and F-Alginate (1:1) (C) in PBS.

Figure 2-4 shows the ^{1}H NMR spectra of alginate, and methine protons on α-D-mannuronic acid and β-L-guluronic acid were confirmed from 3.2–4.1 ppm as a broad peak. After the conjugation, F-Alginate showed peaks from vinylene groups on the furan unit at 6.2, 6.3, and 7.4 ppm.

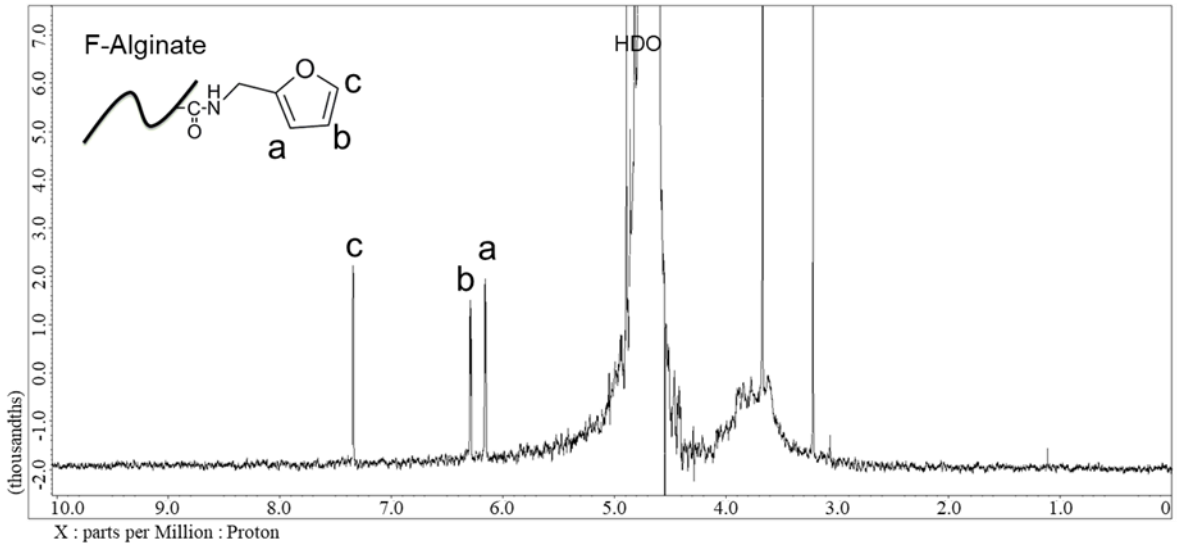

Figure 2-4. ^{1}H NMR spectrum of F-Alginate (solvent: D_2O).

The content of the furan unit was estimated from the relative peak intensity of vinylene groups in furan (3H; 6.2, 6.3 and 7.4 ppm) to phenyl groups in benzyl alcohol (5H; 7.2 ppm) which was added as a reference (Figure 2-5).

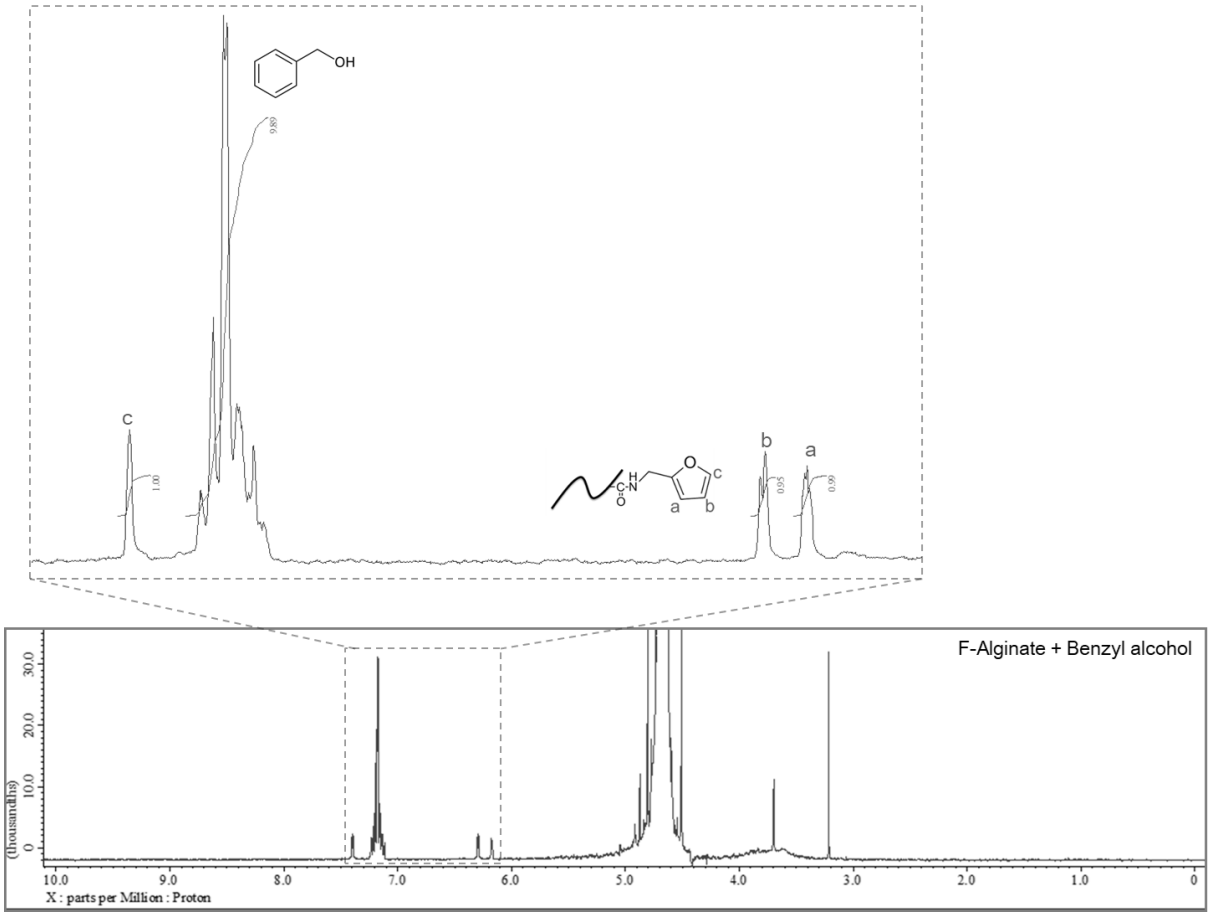

Figure 2-5. The content of furan in F-alginate was evaluated with comparison of benzyl alcohol. The peak at 7.2 ppm corresponds to benzyl alcohol and the furan specific 3 peaks are shown at 6.0 – 8.0 ppm.

Table 2-1 summarizes the result of the furan group content analysis. With an increasing feed concentration of furfurylamine, the furan group content in F-Alginate, which was calculated from the NMR, increased. However, an excess amount of furfurylamine did not increase the content beyond 27–28%. The conjugation was saturated over the stoichiometric condition (1:1).

Table 2-1. Characterization of furan content in F-Alginate.

Sample name	**Feed molar ratio Furfurylamine : COOH**	**Conversion (%)[a]**
F-Alginate (1:2)	1:2	13.2
F-Alginate (1:1)	1:1	27.8
F-Alginate (2:1)	2:1	28.9

[a] The percentage indicates the molar percentage of furan to the carboxylates in alginate.

2.3.2 Photo-curing of F-Alginate

The time course of gel formation of F-Alginate (1:1) in the presence of two photosensitizers, Rose Bengal and riboflavin, during visible light exposure was investigated and the results are shown in Figure 2-6A and 2-6B. The amount of formed gel steadily increased with increased exposure time, and with an increase in the concentration of F-Alginate. A 10% F-Alginate solution achieved over 80% gel formation after a 10 min exposure. Comparing Rose Bengal and riboflavin as photosensitizers, both showed almost the same effect on gel formation.

Figure 2-6C shows the time course of C-Alginate gel formation. The gel formation was faster than that of F-Alginate. Over 20% of the gelation occurred rapidly after the mixing of alginate and calcium, and the gelation ceased after 5 min.

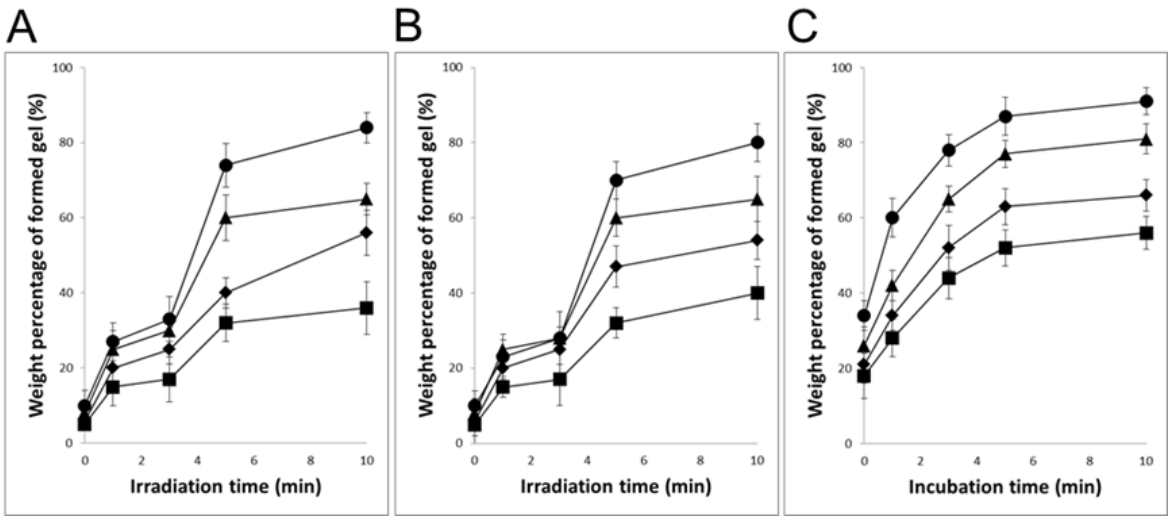

Figure 2-6. Time course of alginate gel formation. (A) F-Alginate (1:1) gel formation in the presence of Rose Bengal. (B) F-Alginate gel formation in the presence of riboflavin. (C) C-Alginate gel formation in the presence of 3.75% $CaCl_2$, which corresponds to the molar percentage of carboxylate groups in alginate. The concentration of F-Alginate (1:1) and that of C-Alginate was 1% (■), 3% (◆), 5% (▲) and 10% (●). n = 3.

2.3.3 Viscoelastic property of alginate hydrogel

The viscoelasticity of the F-Alginate gel is shown in Table 2-2. Before the visible light exposure, the F-Alginate was in a sol state and showed low G' and G'' values. After exposure to visible light for 10 min, both G' and G'' increased. F-Alginate showed a higher G' value than G'' value, which indicated gel formation. The two photosensitizers had the same influence on the gel formation of F-Alginate.

The formed F-Alginate gel was compared with conventional ionic crosslinking using the divalent cationic ion Ca^{2+} (C-Alginate) as shown in Table 2-2

Table 2-2. Viscoelastic properties of ionic and photo-crosslinked 10% alginate[a]

Sample	Irradiation [b]	Additive	G' (Pa)	G" (Pa)
F-Alginate (1:1)	-	-	8.26 ± 3.2	40.1 ± 3.5
	+	%[c] Rose Bengal	366 ± 4.6	164 ± 3.9
		%[c] Riboflavin	339 ± 3.8	135 ± 1.5
C-Alginate	-	1.00%[d] $CaCl_2$	10.8 ± 2.2	29.9 ± 4.8
		2.00%[d] $CaCl_2$	152.6 ± 8.3	62.6 ± 7.8
		3.75%[d] $CaCl_2$	327 ± 2.1	85.0 ± 4.1
		7.50%[d] $CaCl_2$	616.8 ± 7.6	102.6 ± 8.6
		18.75%[d] $CaCl_2$	708.9 ± 8.4	148.4 ± 9.8

[a] Frequency: 1 Hz. Strain 1%, n = 3.

[b] Visible light exposure time: 10 min.

[c] The percentage indicates the w/w percentage of aqueous solution.

[d] The percentage indicates molar percentage of calcium to the carboxylate groups in alginate.

G’ and G’’ depended on the concentration of $CaCl_2$. C-Alginate prepared using 3.75% Ca^{2+} had a similar G’ value as that of F-alginate. Assuming that the crosslinking points can be calculated from the similarity of the G’ value, 3.75% of the carboxylates in the alginate were spent during crosslinking in C-Alginate, and over 10% of furan residues (27% of the carboxylates in the alginate) were calculated to be used during crosslinking in F-Alginate.

When the elastic modulus G’ of the photo-curable systems was compared, it ranged from several hundred kPa to less than one hundred Pa[10, 12-14]. Although a high G’ is required for dental applications, the G’ demonstrated in the present study is enough for soft tissue replacement, taking into consideration the G’ of Ca^{2+}-crosslinked alginate.

Considering that the G’’ of F-Alginate was higher than that of C-Alginate, the F-Alginate gel possesses greater viscosity than C-Alginate. According to a previous study, Ca^{2+}-crosslinked alginate hydrogels form a specific “egg box” structure consisting of a bundle of several alginate polymers created through crosslinking of a large number of α-L-guluronate units[51]. Because of this structure, alginate polymers are considered undergo tight crosslinking to form a stiff hydrogel. In contrast, F-Alginate undergoes crosslinking through the reaction of randomly distributed furan residues. This difference in crosslinking structure is considered to contribute to different hydrogel properties.

2.3.4 Release profile of F-Alginate

Fluorescently labeled dextrans with different molecular weights were incorporated into F-Alginate. Before and after gel formation, the release profile of the molecules was determined (Figure 2-7A and 2-7B). Without light exposure, the incorporated molecules were rapidly released. In contrast, photo- crosslinked F-Alginate slowly released the incorporated molecules. The molecular weight of the molecules affected the release behavior. The smaller molecules were more quickly released from the gel.

Figure 2-7C shows the molecular weight dependence of the released molecules after 12 hours. In addition to dextran, the release of BSA and IGF-1 was plotted in terms of their molecular weight. The proteins were similar to the polysaccharides in terms of the relationship between their molecular weight and release behavior. The result demonstrates that the release profile of alginate simply depends on the molecular weight of the encapsulated substances.

The release of molecules from an alginate hydrogel depends on two factors; one is diffusion, and another involves an interaction with carboxylic acid[52]. In the simple diffusion case, small molecules are rapidly released from the alginate hydrogel within several hours (approximately)[53]. The release of large molecules such as proteins is influenced by the molecular weight of the molecules and they are typically continuously released from the gel for several days to weeks. In addition, the release rate is highly dependent on the interaction between the encapsulated molecules and alginate[54]. In the current study, it was considered that the neutral dextrans and proteins were released without specific interactions with the alginate matrix in accordance with the diffusion mechanism.

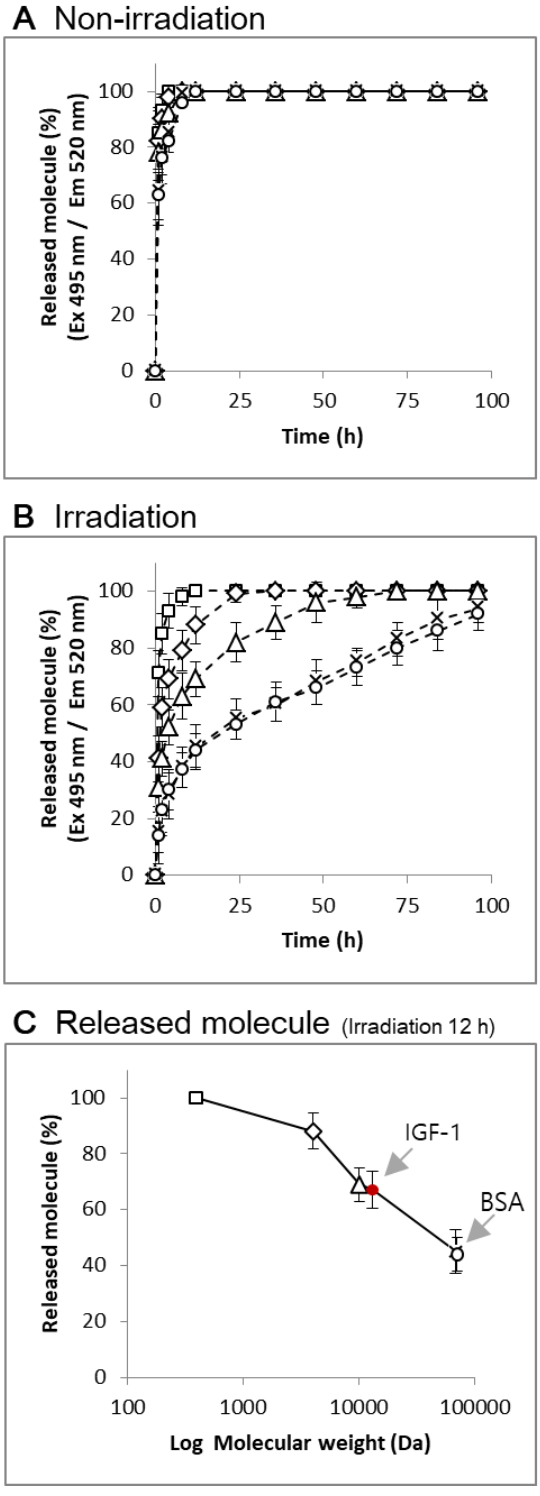

Figure 2-7. Release of FITC 0.39k (□), Dex4k (◇), Dex10k (△), BSA (X) and Dex70k (○) from (A) non-cured and (B) photo-cured F-Alginate (1:1). (C) The relationship between the released amount of incorporated molecules from F-Alginate (1:1) after 12 h and the molecular weight of the molecules. n = 3.

The release behavior of Dex70k from F-Alginate and C-Alginate was compared, as shown in Figure 2-8. The release rate from C-Alginate decreased with an increase in Ca^{2+} concentration, which corresponds to increased crosslinking points. The F-Alginate showed a similar release behavior as C- Alginate prepared using 3.75% $CaCl_2$. However, it is difficult to directly compare the release behavior of these hydrogels, considering that the crosslinking in C-Alginate is ionic and disintegration occurs over time.

Kikuchi et al.[53, 55] and Amsden et al.[56] reported on Ca^{2+}-crosslinked alginate release systems. They reported that the release of Ca^{2+} and the molecular weight and the concentration of alginate significantly affected the release behavior[53]. The release of 145,000 dextran, a high molecular weight molecule, depended on the exchange of Ca^{2+}, and occurred in a "burst" fashion after an initial lag period was observed[55]. The alginate content also affected the release behaviors of protein[56].

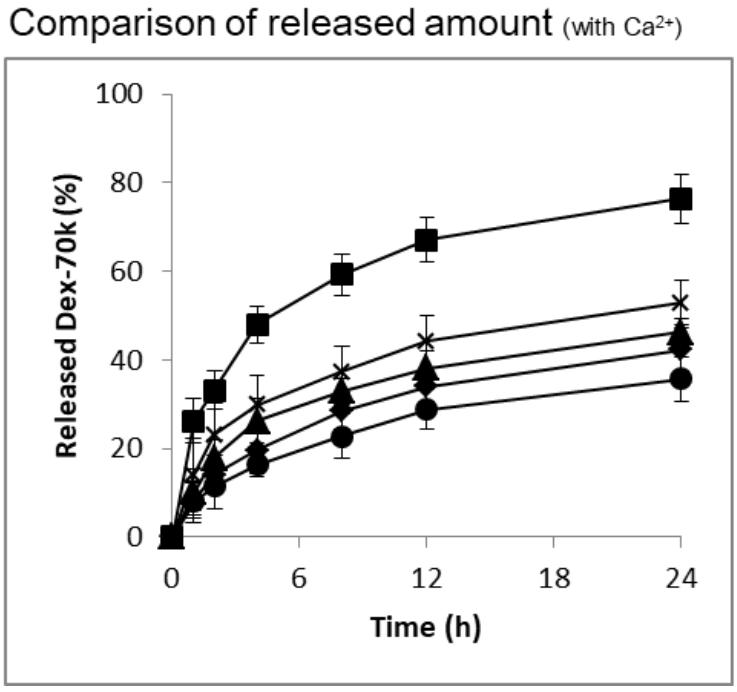

Figure 2-8. Release of Dex70k from alginate hydrogel prepared through photo-curing of F-Alginate (X). C-Alginate with 2% $CaCl_2$ (■), 3.75% $CaCl_2$ (▲), 7.50% $CaCl_2$ (◆) and 18.75% $CaCl_2$ (●). n = 3.

2.3.5 Cytotoxicity of photo-sensitizers

Rose Bengal is used for food staining and in drugs, and riboflavin is a vitamin (vitamin B2). Therefore, these photosensitizers are a good candidate for medical applications. However, the lethal dose (LD50) of Rose Bengal and riboflavin for 3T3 cells was measured to be 8.6 and 34.2 μM, respectively (Figure 2-8). A similar cytotoxicity was reported previously[36]. Therefore, the samples were washed prior to cell culture experiments.

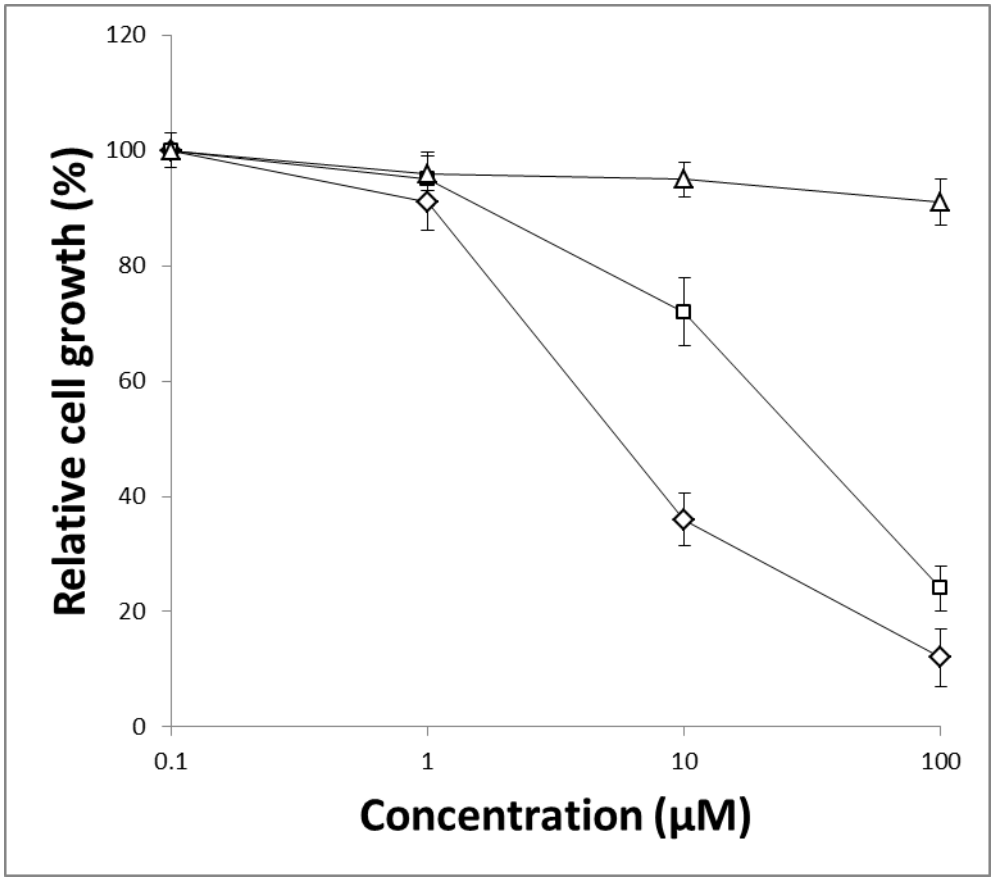

Figure 2-8. Relative cell growth of NIH/3T3 cells when exposed to photo-sensitizers. Alginate (△), Rose Bengal (◇) and riboflavin (□). Relative cell growth means the comparison of seeded cell number. n=3.

The cell growth enhancement percentage in the present study was two times as high as that in our previous report[39]. Since the previous study employed too high density of seeded cells (three times as high as the present study), the growth curve was close to the saturated region (Figure 2-9). Therefore, the present study adjusted the density of seeded cell to clearly show the effect.

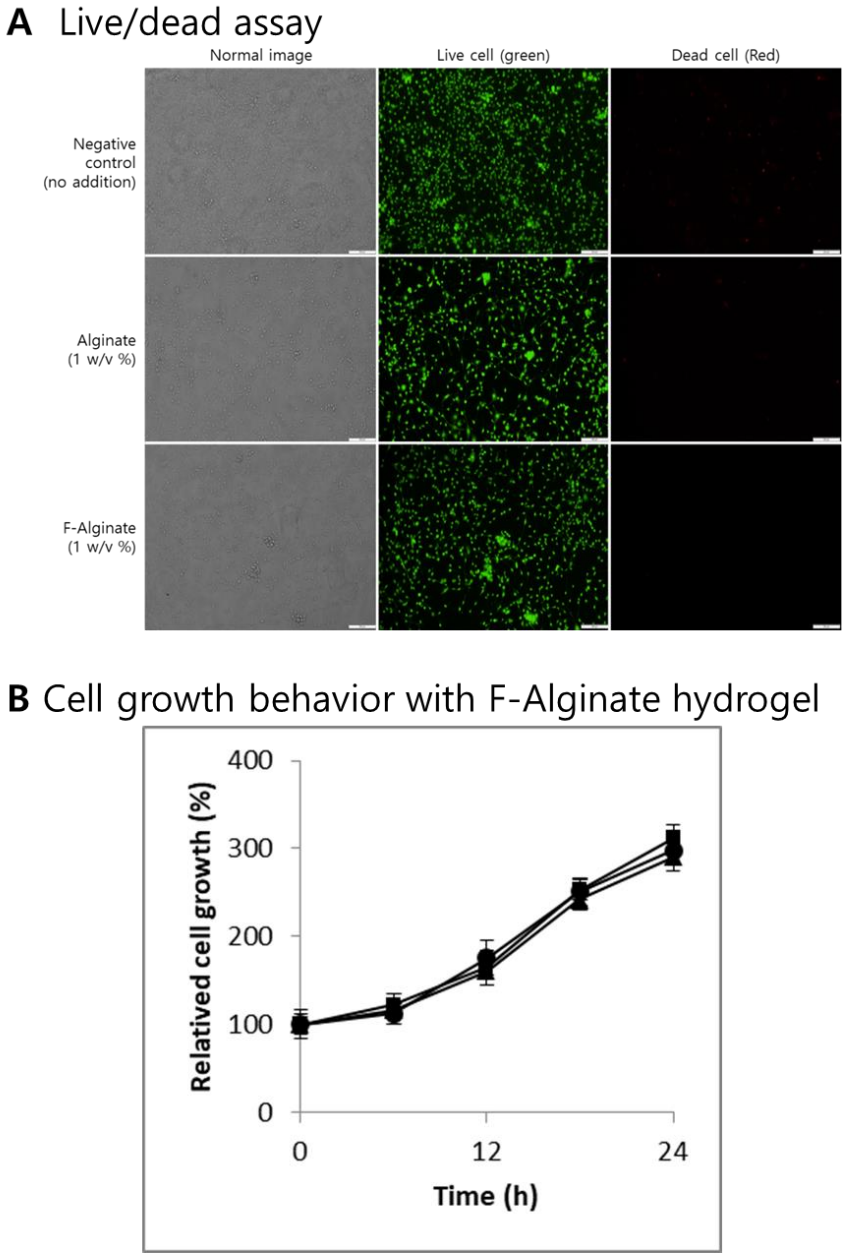

Figure 2-9. (A) Phase contrast and fluorescence images of cells in the presence of non-crosslinked alginate or F-Alginate. The green and red signals derived from calcein AM and ethidium homodimer-1, respectively. The scale bars are 200 μm. (B) Cell growth behavior of the NIH/3T3 cells with the F-Alginate hydrogel. The hydrogel was washed using PBS prior to cell culture. Relative cell growth means a comparison of the seeded cell numbers ($1x10^4$ cells/mL) (■: no addition, ▲: F-Alginate with Rose Bengal, and ●: F-Alginate with riboflavin). n = 3.

2.3.6 Released IGF effect on cell growth

IGF-1 release from the alginate hydrogel was investigated in the present study. The cells were cultured in medium containing 5% FBS. The addition of IGF-1 enhanced cell growth, as shown in Figure 2-10A. The release of IGF-1 was monitored, as shown in Figure 2-10B. Figure 2-10C shows the effect of the continuous release of IGF-1 on cell growth.

The results show that the batch addition of 50 ng/mL IGF-1 had almost the same effect as an F- alginate hydrogel containing 20 ng/mL IGF-1 during the initial 12 h. As shown in Figure 6B, the amount of released IGF-1 was calculated to be 8.62 ± 0.74 ng/mL. This indicates that the continuous addition of a small amount of growth factor is as effective as one high concentration batch addition. The low concentration of growth factor may have efficiently enhanced cell growth without down- regulating the signaling mechanism.

After 24 hours of culture since the culture medium was changed, the growth rate in the absence of F- Alginate returned to that of untreated cells. However, the growth rate in the presence of F-Alginate containing IGF-1 was continuously high. This was likely caused by the continuous release of IGF-1 from the F-Alginate gel.

Recently, we are developing a 3D bioprinting system using furfulyl gelatin[57, 58]. In future, 3D cell culture using visible light (not ultraviolet light)-sensitive materials will become more important for tissue engineering[59].

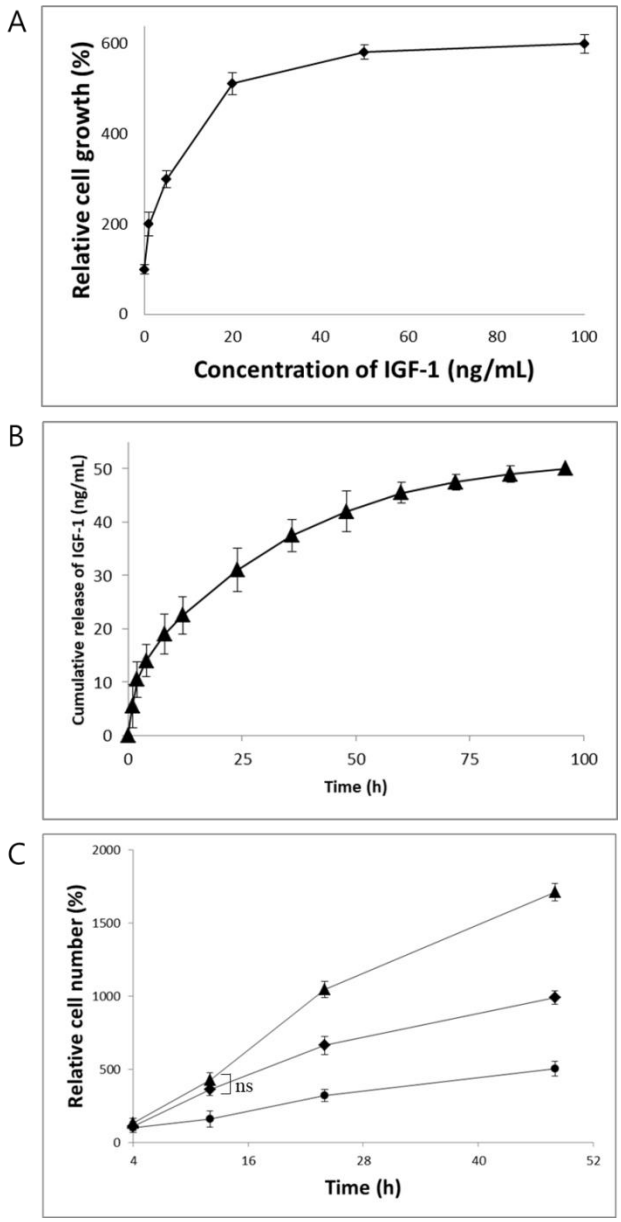

Figure 2-10. (A) Relative cell growth of NIH/3T3 cells with various concentrations of IGF-1 at 24 h. (B) Release profile of IGF-1 from a series of photo-cured 10% F-Alginate (1:1) hydrogel samples (▲). (C) Relative cell growth with 10% F-Alginate with IGF-1 (20 ng/mL) before or after irradiation with visible light for 10 min at 40℃ (◆: F-Alginate with IGF-1 before irradiation, ▲: F-Alginate with IGF-1 after irradiation and ●: no addition). Relative cell growth means the comparison of seeded cell numbers at 4 h. n = 3. ns = no significant difference.

2.4 Conclusion

Furan-conjugated alginate was prepared and photo-crosslinked in the presence of Rose Bengal or riboflavin photosensitizers. The mechanical and release properties of the visible light-induced gel were similar to that of conventional Ca^{2+}-induced crosslinked alginate. This type of visible-light sensitive materials will be important for tissue engineering.

2.5 References

1. Y. Ito, Photochemistry for biomedical applications: from device fabrication to diagnosis and therapy, *Springer*, 2018.

2. D. Zhou, Y. Ito, Visible light-curable polymers for biomedical applications. *Science China Chemistry*, 57, 510-521, 2014.

3. S. Kurata, N. Yamazaki, New matrix polymers for photo-activated resin composites using di-α-fluoroacrylic acid derivatives, *Dental Materials Journal*, 27, 534-540, 2008.

4. X. Miao, Y. Li, Q. Zhang, M. Zhu, H. Wang, Low shrinkage light curable dental nanocomposites using SiO_2 microspheres as fillers, *Materials Science and Engineering: C*, 32, 2115-2121, 2012.

5. A. Vitale, M. Sangermano, R. Bongiovanni, P. Burtscher, N. Moszner. Visible light curable restorative composites for dental applications based on epoxy monomer, *Materials*, 7, 554-562, 2014.

6. T. Matsuda, J. Nagase, A. Ghoda, Y. Hirano, S. Kidoaki, Y. Nakayama, Phosphorylcholine-endcapped oligomer and block co-oligomer and surface biological reactivity, *Biomaterials*, 24, 4517-4527, 2003.

7. H.K. Park, M.K. Shin, B.K. Kim, J.W. Park, H.S. Lee, A visible light-curable yet visible wavelength-transparent resin for stereolithography 3D printing, *NPG Asia Materials*, 10, 82-89, 2018.

8. X. Li, S. Chen, J. Li, X. Wang, J. Zhang, N. Kawazoe, G. Chen, 3D culture of chondrocytes in gelatin hydrogels with different stiffness, *Polymers*, 8, 1-15, 2016.

9. J.C. Liu, I.Y. Rad, F. Sun, J.W. Stansbury. Photo-reactive nanogels as a means to tune properties during polymer network formation, *Polymer Chemistry*, 5, 227-233, 2014.

10. L. Cai, C.J. Foster, X. Lui, S. Wang, Enhanced bone cell functions on poly (ε-caprolactone) triacrylate networks grafted with polyhedral oligomeric silsesquioxane nanocages, *Polymer*, 55, 3836-3845, 2014.

11. X. Nan, Y. Huang, J. Shao, H. Yan, M. Wu, Y. Yao, Co-initiating function of silk peptide in free radical photopolymerization, *Polymer Engineering & Science*, 58, 2185-2191, 2018.

12. S.Y. Kim, Z.K. Cui, J. Fan, A. Fartash, T.L. Aghaloo, M. Lee, Photocrosslinkable chitosan hydrogels functionalized with the RGD peptide and phosphoserine to enhance osteogenesis, *Journal of Materials Chemistry B*, 4, 5289-5298, 2016.

13. Y.B. Yoo, H. Hyun, S.J. Yoon, S.Y. Kim, D.W. Lee, S.W. Um, S. Hong, D.H. Yang, Visible light-cured glycol chitosan hydrogel dressing containing endothelial growth factor and basic fibroblast growth factor accelerates wound healing in vivo, *Journal of Industrial and Engineering Chemistry*, 67, 365-372, 2018.

14. S.J. Yoon, H. Hyun, D.W. Lee, D. Yang, Visible light-cured glycol chitosan hydrogel containing a beta-cyclodextrin-curcumin inclusion complex improves wound healing in vivo, *Molecules*, 22, 1-16, 2017.

15. H. Hyun, M. Park, G.Y. Jo, S. Kim, H. Chun, D.H. Yang, Photo-cured glycol chitosan hydrogel for ovarian cancer drug delivery, *Marine Drugs*, 17, 1-12, 2019.

16. Y. Heo, E.H. Kim, E. Kobatake, J.W. Nah, Y. Ito, T.I. Son, Preparation of phosphonated gelatin-coated titanium containing rhBMP-2 by UV irradiation for improved osteoinduction and function, *Journal of Industrial and Engineering Chemistry*, 36, 66-73, 2016.

17. X. Zhang, C. Jiang, M. Cheng, Y. Zhou, X. Zhu, J. Nie, Y. Zhang, Q. An, F. Shi, Facile method for the fabrication of robust polyelectrolyte multilayers by post-photo-cross-linking of azido groups, *Langmuir*, 28, 7096-7100, 2012.

18. Y. Ito, H. Hasuda, T. Yamauchi, N. Komatsu, K. Ikebuchi, Immobilization of erythropoietin to culture erythropoietin-dependent human leukemia cell line, *Biomaterials*, 25, 2293-2298, 2004.

19. X. Ren, J. Akimoto, H. Miyatake, S. Tada, L. Zhu, H. Mao, T. Isoshima, S. Mueller, S.M. Kim, Y. Zhou, Y. Ito, Cell migration and growth induced by photo-immobilised vascular endothelial growth factor (VEGF) isoforms, *Journal of Materials Chemistry B*, 7, 4272-4279, 2019.

20. D.W. Ham, T.I. Son, T.J. Lee, K.S. Song. Osteogenic effectiveness of photo-immobilized bone morphogenetic protein-2 using different azidophenyl-natural polymer carriers in rat calvarial defect model. *International Journal of Biological Macromolecules*, 121, 333-341, 2019.

21. T. Konno, H. Hasuda, K. Ishihara, Y. Ito, Photo-immobilization of a phospholipid polymer for surface modification, *Biomaterials*, 26, 1381-1388, 2005.

22. K. Ishihara, K. Fukazawa, Y. Inoue, J. Koyama, Y. Mori, T. Kinoshita, K. Hiranuma, N. Yasuda. Reliable surface modification of dental plastic substrates to reduce biofouling with a photoreactive phospholipid polymer, *Journal of Applied Polymer Science*, 135, 1-7, 2018.

23. G. Becker, Z. Deng, M. Zober, M. Wagner, K. Lienkamp, F.R. Wurm. Surface-attached poly(phosphoester)-hydrogels with benzophenone groups, *Polymer Chemistry*, 9, 315-326, 2018.

24. J. Raphel, J. Karlsson, S. Galli, A. Wennerberg, C. Lindsay, M. Haugh, J. Pajarinen, S.B. Goodman, R. Jimbo, M. Andersson, S.C. Heilshorn. Engineered

protein coatings to improve the osseointegration of dental and orthopaedic implants, *Biomaterials*, 83, 269-282, 2016.

25. G. Kaur, P. Johnston, K. Saito, Photo-reversible dimerisation reactions and their applications in polymeric systems, *Polymer Chemistry*, 5, 2171-2186, 2014.

26. B.V. Bochove, D.W. Grijpma. Photo-crosslinked synthetic biodegradable polymer networks for biomedical applications. *Journal of Biomaterials Science Polymer Edition*, 30, 77-106, 2019.

27. W. Dong, J. Ren, L. Lin, D. Shi, Z. Ni, M. Chen, Novel photocrosslinkable and biodegradable polyester from bio-renewable resource, *Polymer Degradation and Stability*, 97, 578-583, 2012.

28. Y. Heo, S.H. Park, S.Y. Seo, J.Y. Yun, Y. Ito, T.I. Son, Preparation and in vivo evaluation of photo-cured O-carboxymethyl chitosan micro-particle for controlled drug delivery, *Macromolecular Research*, 22, 541-548, 2014.

29. B.K. Armstrong, A. Kricker, The epidemiology of UV induced skin cancer, *Journal of Photochemistry and Photobiology B*, 63, 8-18, 2001.

30. F.R. de Gruijl, H.J. Van Kranen, L.H. Mullenders, UV-induced DNA damage, repair, mutations and oncogenic pathways in skin cancer, *Journal of Photochemistry and Photobiology B*, 63, 19-27, 2001.

31. G.P. Pfeifer, A. Besaratinia, UV wavelength-dependent DNA damage and human non-melanoma and melanoma skin cancer, *Photochemical & Photobiological Sciences*, 11, 90-97, 2012.

32. E.H. Kim, G.D. Han, S.H. Noh, J.W. Kim, J.G. Lee, Y. Ito, T.I. Son, Photo-reactive natural polymer derivatives for medical application, *Journal of Industrial and Engineering Chemistry*, 54, 1-13, 2017.

33. M.O. de Beeck, A. Madder. Sequence specific DNA cross-linking triggered by visible light, *Journal of the American Chemical Society*, 134, 10737-10740, 2012.

34. T.I. Son, M. Sakuragi, S. Takahashi, S. Obuse, J.H. Kang, M. Fujishiro, Y. Ito, Visible light-induced crosslinkable gelatin, *Acta Biomaterialia*, 6, 4005-4010, 2010.

35. S.H. Park, S.Y. Seo, H.J. Lee, H.N. Na, J.W. Lee, H.D. Woo, T.I. Son, Preparation of furfuryl-fish gelatin (Ff. gel) cured using visible-light and its application as an anti-adhesion agent, *Macromolecular Research*, 20, 842-846, 2012.

36. E.H. Kim, J.W. Kim, G.D. Han, S.H. Noh, J.H. Choi, M.K. Kim, J.W. Nah, T.Y. Kim, Y. Ito, T.I. Son, Biocompatible, drug-loaded anti-adhesion barrier using visible-light curable furfuryl gelatin derivative, *International Journal of Biological Macromolecules*, 120, 915-920, 2018.

37. S.W. Kim, J.W. Kim, S.H. Noh, E.H. Kim, Y. Ito, J.W. Nah, T.I. Son, Application of visible light curable furfuryl-low molecular chitosan derivative as an anti-adhesion agent, *Journal of Industrial and Engineering Chemistry*, 66, 438-455, 2018.

38. S.H. Park, E.H. Kim, H.J. Lee, Y. Heo, Y.M. Cho, S.Y. Seo, T.Y. Kim, H.W. Suh, M.K. Kim, Y. Ito, J.W. Nah, T.I. Son, Wound healing effect of visible light-curable chitosan with encapsulated EGF, *Macromolecular Research*, 24, 336-241, 2016.

39. Y. Heo, H.J. Lee, E.H. Kim, M.K. Kim, Y. Ito, T.I. Son, Regeneration effect of visible light-curing furfuryl alginate compound by release of epidermal growth factor for wound healing application, *Journal of Applied Polymer Science*, 131, 1-11, 2014.

40. S.H. Noh, S.W. Kim, J.W. Kim, T.H. Lee, J.W. Nah, Y.G. Lee, M.K. Kim, Y. Ito, T.I. Son, Preparation of drug-immobilized anti-adhesion agent using visible light-curable alginate derivative containing furfuryl group, *International Journal of Biological Macromolecules*, 121, 301-308, 2019.

41. G.D. Han, J.W. Kim, S.H. Noh, S.W. Kim, E.C. Jang, J.W. Nah, T.I. Son, Potent anti-adhesion agent using a drug-eluting visible-light curable hyaluronic acid derivative, *Journal of Industrial and Engineering Chemistry*, 70, 204-210, 2019.

42. C.V. Montes, H. Memczak, E. Gyssels, T. Torres, A. Madder, R.J. Schneider, Photoinduced cross-linking of short furan-modified DNA on surfaces, *Langmuir*, 33, 1197-1201, 2017.

43. L.L. Carrette, E. Gyssels, N. de Laeta, A. Madder, Furan oxidation based cross-linking: a new approach for the study and targeting of nucleic acid and protein interactions, *Chemical Communications*, 52, 1539-1554, 2016.

44. S.A. Kumar, S.C. Allen, N. Tasnim, T. Akter, S.H. Park, A. Kumar, M. Chattopadhyay, Y. Ito, L.J. Suggs, B. Joddar. The applicability of furfuryl-gelatin as a novel bioink for tissue engineering applications, *Journal of Biomedical Materials Research Part B: Applied Biomaterials*, 107B, 314-323, 2019.

45. S.A. Kumar, N. Tasnim, E. Dominguez, S. Allen, L. Suggs, Y. Ito, B. Joddar, A comparative study of a 3D bioprinted gelatin-based lattice and rectangular-sheet structures, *Gels*, 4, 11-12., 2018.

46. J.C. Lui, M. Colbert, C.S.F. Cheung, M. Ad, A. Lee, Z. Zhu, K.M. Barnes, D.S. Dimitrov, J. Baron, Cartilage-targeted IGF-1 treatment to promote longitudinal bone growth, *Molecular Therapy*, 27, 670-680, 2019.

47. H.T. Jiang, C.C. Ran, Y.P. Liao, J.H. Zhu, H. Wang, R. Deng, M. Nie, B.C. He, Z.L. Deng, IGF-1 reverses the osteogenic inhibitory effect of dexamethasone on BMP9-induced osteogenic differentiation in mouse embryonic fibroblasts via

PI3K/AKT/COX-2 pathway, *Journal of Steroid Biochemistry and Molecular Biology*, 191, 105363, 2019.

48. Z. Zhang, L. Li, W. Yang, Y. Cao, Y. Shi, X. Li, Q. Zhang, The effects of different doses of IGF-1 on cartilage and subchondral bone during the repair of full-thickness articular cartilage defects in rabbits, *Osteoarthritis and Cartilage*, 25, 309-320, 2017.

49. H.L. Wagner, The Mark–Houwink–Sakurada equation for the viscosity of atactic polystyrene, *Journal of Physical and Chemical Reference Data*, 14, 1101-1106, 1985.

50. I. Kagawa, A. Takahashi, Studies on polymer electrolyte, *Journal of the Chemical Society of Japan*, 56, 252-253, 1953.

51. G.T. Grant, E.R. Morris, D.A. Rees, P.J. Smith, D. Thom, Biological interactions between polysaccharides and divalent cations: the egg-box model, *Federation of European Biochemical Societies letters*, 32, 195-198, 1973.

52. K.Y. Lee, D.J. Mooney, Alginate: properties and biomedical applications, *Progress in Polymer Science*, 37, 106-126, 2012.

53. A. Kikuchi, M. Kawabuchi, A. Watanabe, M. Sugihara, Y. Sakurai, T. Okano, Effect of Ca^{2+}-alginate gel dissolution on release of dextran with different molecular weights, *Journal of Controlled Release*, 58, 21-28, 1999.

54. K.Y. Lee, M.C. Peters, D.J. Mooney, Comparison of vascular endothelial growth factor and basic fibroblast growth factor on angiogenesis in SCID mice, *Journal of Controlled Release*, 87, 49-56, 2003.

55. A. Kikuchi, M. Kawabuchi, M. Sugihara, Y. Sakurai, T. Okano, Pulsed dextran release from calcium-alginate gel beads, *Journal of Controlled Release*, 47, 21-29, 1997.

56. B. Amsden, N. Turner, Diffusion characteristics of calcium alginate gels, *Biotechnology and Bioengineering*, 65, 605-610, 1999.

57. S.A. Kumar, M. Alonza, S. Allen, L. Abelseth, V. Thakur, J. Akimoto, Y. Ito, S. Willerth, L. Suggs, M. Chattopadhyay, B. Joddar, A visible light crosslinkable, fibrin-gelatin based bioprinted cardiac construct with human cardiomyocytes and fibroblasts, *ACS Biomaterials Science & Engineering*, 5, 4551-4563, 2019.

58. S.A. Kumar, N. Tasnim, E. Dominguez, S. Allen, L. Suggs, Y. Ito, B. Joddar, A comparative study of a 3D bioprinted gelatin-based lattice and rectangular-sheet structures, *Gels*, 4, 73, 2018.

59. S. Sakai, H. Kamei, T. Mori, T. Hotta, H. Ohi, M. Nakahata, M. Taya, Visible light-induced hydrogelation of an alginate derivative and application to stereolithographic bioprinting using a visible light projector and acid red, *Biomacromolecules*, 19, 672-679, 2018.

CHAPTER 3

IMMOBILIZATION OF IGF

3.1 Introduction

Various materials including organic and inorganic components have been used as biomaterials widely in medical fields due to their mechanical property, nontoxicity and biocompatibility[1, 2]. For the applications, various studies have reported surface modification of biomaterials[3-5]. One of the aims of surface modification is an addition of biological functions on the biomaterials.

For the surface alteration, various molecules such as polymer and protein have been immobilized on material surfaces[6-8]. To use the materials in human body, cell adhesiveness and non-biofouling have been studied by coating of active peptide and extracellular matrix[9-12]. Additionally, the immobilization of protein on surface was also investigated to control higher levels of cell functions such as growth and differentiation[13, 14].

Growth factors are involved in cell growth, proliferation and differentiation and bind to specific receptors to show their respective functions[15-17]. Recent studies have found that chemical immobilization of growth factor proteins enabled the biomaterials mitogenic[18-20]. However, there is still a limitation to immobilization, such as requirement of chemical treatment of material surfaces, that is difficult to inorganic materials. Therefore, here an adhesive polypeptide containing the mitogenic activity was developed[21, 22].

It is known that marine mussels rapidly, strongly, and toughly attach to various solid surfaces in the sea, otherwise they will be dislodged and dashed by the waves[23, 24]. The holdfast mechanism has provided important and physical insights into moisture-resistant adhesion. 3,4-Dihydroxyphenylalanine (DOPA) was found in the mussel adhesion proteins and plays important roles in adhesion to various materials,

including polymers, metals and ceramics[25, 26]. Inspired from this finding, various functional polymers carrying DOPA derivatives have been developed to provide diverse adhesive, sealant, and anchoring properties[27, 28].

In this study, an active domain of IGF-1 sequence was conjugated to a DOPA-containing peptide sequence (IGF-DOPA) for immobilization of active IGF on typical organic and inorganic material surfaces such as titanium and polystyrene. The IGF-DOPA was bound onto the material surfaces and they exhibited the biological activity with cell growth.

3.2 Materials and methods

3.2.1 Materials

IGF-1 (Minneapolis, MN, USA) was purchased from R&D Systems. Titanium plates (Osaka Vacuum Industries, Osaka, Japan) were prepared using 400 nm electron beam by vacuum deposition of titanium onto glass plate (1 mm in thickness and 15 mm in diameter, Matsunami Glass Ind.,Ltd., Osaka, Japan). The plates were washed by ultrasonication in hexane, 6M HCl, ultrapure water, 70% EtOH and PBS, respectively. Finally, they were irradiated with UV for 15 min before each experiment. Cell culture plates (BD Falcon, NY, USA) were used as polystyrene surfaces without further treatments.

3.2.2 Preparation of IGF-DOPA

Peptide sequences with DOPA (DOPA-Lysine-DOPA-Lysine-DOPA-Glycine, XKXKXG; X represents DOPA) were prepared by the solid-phase peptide synthesis method. Truncated IGF-1 with the binding sequence at the C-terminus was synthesized with the method using 9-fluorenylmethoxycarbonyl (Fmoc) protected amino acids by Support Unit for Bio-Material Analysis at RIKEN. Low density of amino acid-loaded resin Fmoc-Gly-NovaSyn® TGT (0.2 mmol/g) was purchased from Novabiochem® (San Diego, CA, USA). In addition to conventional Fmoc-protected canonical amino acids, Fmoc-DOPA (acetonide)-OH (Merck, Darmstadt, Germany) was used. The peptide synthesizer ABI433A (Thermo Fisher Scientific, Waltham, MA USA) was employed. After purification using high performance liquid chromatography (HPLC) equipped with a Hipep-Intrada RP C18 column (150 × 4.6 mm I.D.), the formulations of the peptide were measured by matrix-assisted laser desorption/ionization-time-of-flight mass analysis (MALDI-TOF MS) on a microflex (Bruker Daltonics K.K., Billerica, MA USA). The synthesized IGF derivative was referred to as IGF-DOPA.

For refolding of IGF-DOPA three kinds of buffers were employed. (1) Solubilizing buffer; 50 mM MES (pH 6.0), 1 M NaH_2PO_4, 6M guanidine hydrochloride and 10 mM 2-mercaptoethanol, (2) refolding buffer; 50 mM MES (pH 6), 200 mM NaCl, 1 mM EDTA, 0.2 mM GSSG (oxidized glutathione) and 1 mM GSH (Reduced Glutathione), and (3) replacing buffer; 50 mM MES (pH 6) and 10 % (v/v) glycerol buffer. The synthesized IGF-DOPA was dissolved in the solubilizing buffer and the solution was diluted with refolding buffer. After the refolding, IGF-DOPA solution was exchanged with replacing buffer. The sample was concentrated by centrifugation and freeze-dried for biological activity assays.

3.2.3 Binding assay

The binding affinity of IGF-DOPA peptide to material surfaces was measured at room temperature using a quartz crystal microbalance with dissipation monitoring (QCM-D, Meiwafosis Co., Ltd., Tokyo, Japan). The buffer was allowed to run for stabilization of the baseline. Subsequently the samples of different concentrations (1, 5, 25 and 50 μg/mL) were loaded into the measurement system and kept running at 65 μL/min for 15 min. The substrate was washed by running buffer solution and Milli-Q water. Measurements were performed at three times under same condition and the average value was calculated.

3.2.4 Biological activity of immobilized IGF-DOPA

NIH/3T3 and MC3T3-E1 cells were cultured in Dulbecco's modified Eagle's medium (DMEM, Wako Pure Chemical Industries, Ltd., Osaka, Japan) and minimum essential medium Eagle -alpha modification (MEMα, Wako Pure Chemical Industries, Ltd., Osaka, Japan), respectively. Both cells were cultured with 1% penicillin-streptomycin (Nacalai Tesque, Inc., Kyoto, Japan) and 10% fetal bovine serum (FBS, MP Biomedicals, LLC., Illkirch, France) at 37 °C in 95% humidified air with 5% CO_2. The cultured cells were washed using 6 mL of PBS and harvested with 0.25% trypsin solution containing 1 mM EDTA at 37 °C for 2 min. The recovered cells were suspended in medium for *in vitro* cell experiments.

IGF-DOPA solutions were bound onto titanium and polystyrene surfaces for 30 min at 37 °C and washed with PBS three times for 5 min. The suspended cells were seeded on the surfaces and cultured at 37 °C in 5% CO_2 atmosphere condition.

The cell proliferation was quantified with a cell counting kit-8 (CCK-8, Dojindo, Tokyo, Japan) using WST-8. WST-8 solutions were added to the culture medium for NIH/3T3 cells and cells were incubated for 2 h at 37 ℃ in a humidified atmosphere containing 5% CO_2. The absorbance of the medium at 450 nm was measured using a microplate reader (EnSpire Alpha 2390; Perkin-Elmer, Waltham, MA, USA).

For osteogenesis induction, ascorbic acid (25 μg/mL) and glycerophosphate (5 mM) was added to culture medium for MC3T3-E1 cells. The cell differentiation was investigated using Alizarin Red S (ARS) staining assay (Ared-Q, ScienCell Research Laboratories, CA, USA). After the culture of MC3T3-E1 cells, the medium was removed and washed using PBS. The cells were fixed with 4% paraformaldehyde solution for 15 min at room temperature. After washing with Milli-Q water, 40 mM ARS solution was added and incubated at room temperature for 30 min. The dye was removed and the cells were washed five times with Milli-Q water. To extract the dye, 10% acetic acid was added and incubated for 30 min at room temperature. The solutions were collected to 1.5 mL tubes and heated at 85 ℃ for 10 min. The samples were incubated on ice for 5 min. After centrifugation at 20,000 g for 15 min, supernatants were transferred to new tubes and mixed with 10% ammonium hydroxide. Finally, the absorbance of the samples was measured at 405 nm.

Cell differentiation marker was measured by the western blot. For the measurement, the cell lysate was prepared with lysis buffer containing 50 mM Tris-HCl (pH 7.0), 150 mM NaCl, 1 mM EDTA, 1% NP40 and complete protease inhibitor cocktail (Merck) on ice. The samples were centrifuged at 15,000 rpm for 15 min at 4℃. The concentration of supernatant (protein) was measured by BCA assay (Thermo Fisher Scientific). The samples were mixed with the buffer containing 1 mM Tris-HCl (pH 6.8), 50% glycerol, 20% SDS and 5% β-mercaptoethanol and they were heated

for 5 min at 95℃. The treated sample was applied onto SDS-PAGE conducted for 57 min at 200 V / 40 mA, and the proteins were transferred to immobilon transfer polyvinylidene difluoride membrane (Merck) for 30 min at 25 V. The membrane was blocked with ECL prime blocking agent (GE Healthcare Life Sciences, New Jersey, USA) for 30 min at room temperature. The membrane was washed 3 times for 5 min with TBS-T. The antibodies for each marker [Bovine Osteocalcin mouse monoclonal antibody (QED Bioscience, California, USA), Osteoponin mouse monoclonal antibody (Santa Cruz Biotechnology, California, USA) and β-actin mouse monoclonal antibody (Cell Signaling Technology, Massachusetts, USA)] were added. After the membranes were washed with TBS-T for 10 min and incubated with polyclonal rabbit anti-mouse immunoglobulins/HRP (Dako, Glostrup, Denmark) for 1 hr at room temperature. Finally, ECL detection reagent (GE Healthcare Life Science) was added on the membrane and the image was analyzed by luminograph II (WSE-6200H, ATTO, Tokyo, Japan).

3.3 Results and discussion

3.3.1 Preparation of IGF-DOPA

IGF-1 sequence reported by Sandberg-Nordqvist et al.[29] was employed in this study. The deletion of three amino acids at the N-terminal was reported to reduce its biological activity, although it locates in the body[30]. On the other hand, the modification of both of the N- and C- terminals kept the activity of IGF-1[31].

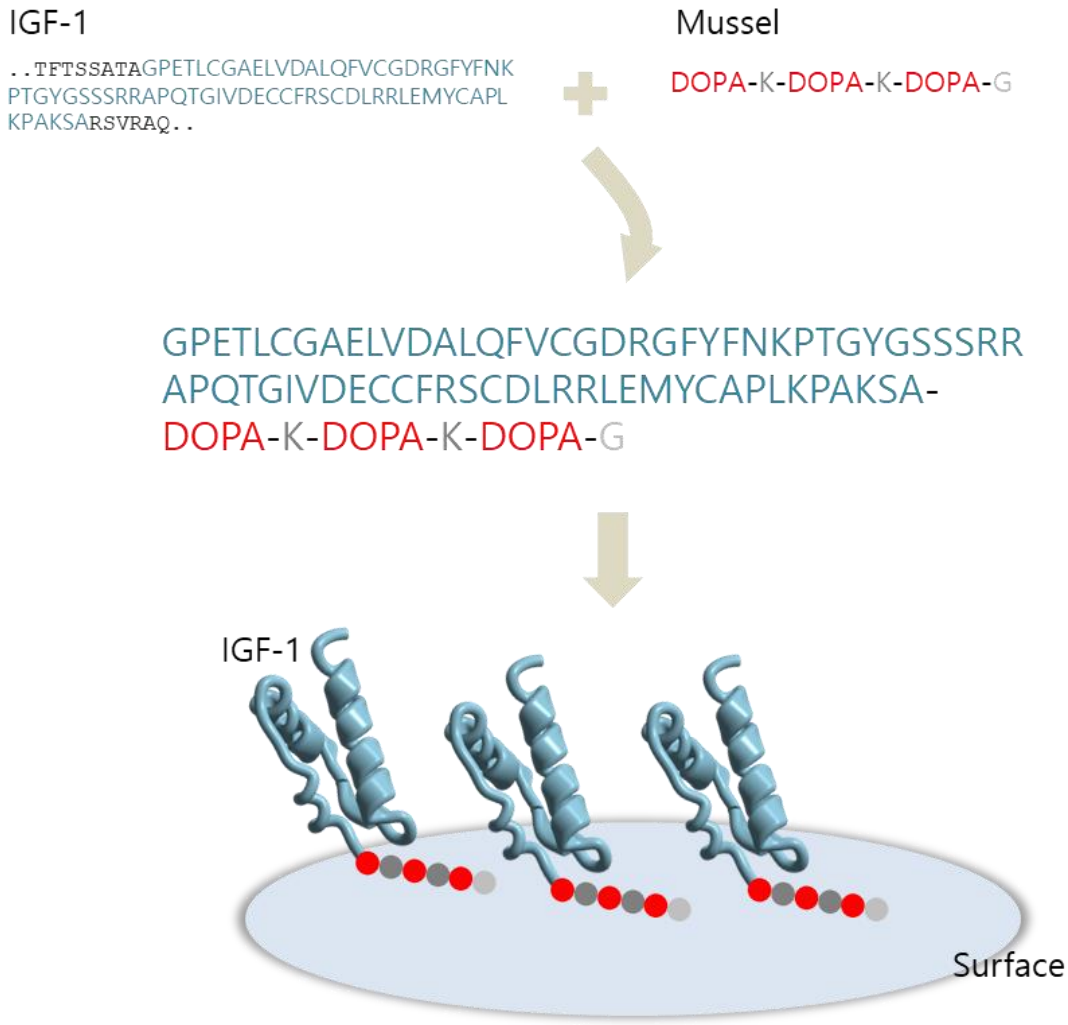

Figure 3-1. Peptide sequence of IGF-DOPA.

Therefore, in this study we conjugated the binding peptide on the C-terminal of IGF-1 without modification (Figure 3-1). The binding sequence DOPA-KDOPA-K-DOPA-G was designed according to Messersmith's studies[32].

The purity of synthesized IGF-DOPA peptide was confirmed using HPLC analysis (Figure 3-2). Since MALDI TOF-MS peak position was calculated for IGF-DOPA ($C_{372}H_{573}N_{102}O_{113}S_7$) m/z $[M+H]^+$ 8506.7 (Av.), and found m/z $[M+H]^+$ 8506.2 (Av.), the synthesis was confirmed.

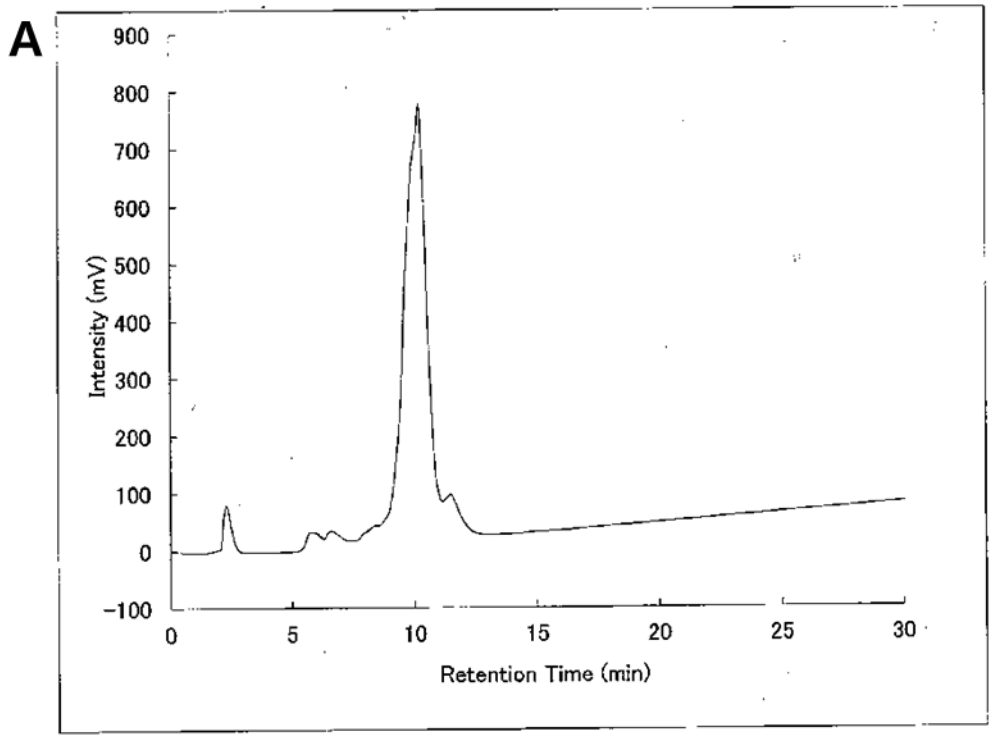

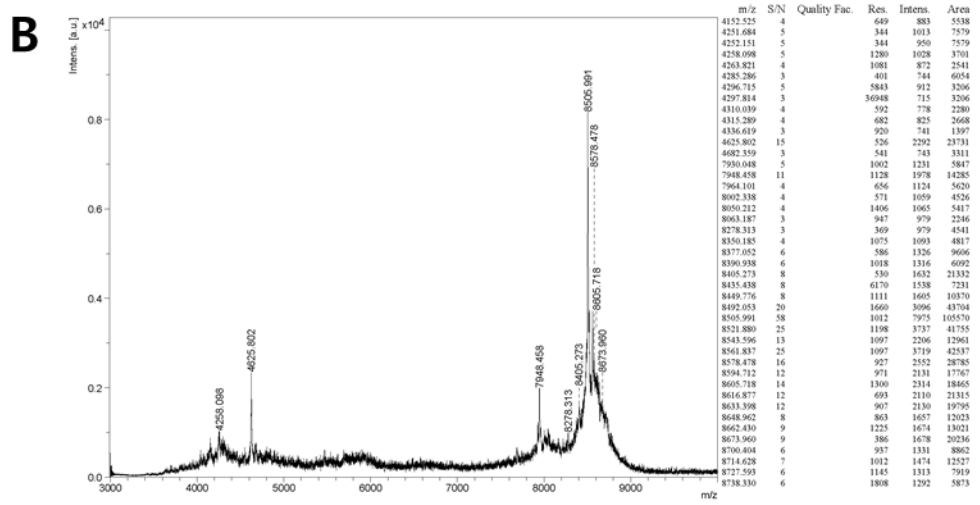

m/z	S/N	Quality Fac.	Res.	Intens.	Area
4152.525	4		649	883	5538
4251.684	5		344	1013	7579
4252.151	5		344	950	7579
4258.098	5		1280	1028	3701
4263.821	4		1081	872	2541
4285.286	3		401	744	6054
4296.715	5		5843	912	3206
4297.814	3		36948	715	3206
4310.039	4		592	778	2280
4315.289	4		682	825	2668
4336.619	3		920	741	1397
4625.802	15		526	2292	23731
4682.359	3		541	743	3311
7930.048	5		1002	1231	5847
7948.458	11		1128	1978	14285
7964.101	4		656	1124	5620
8002.338	4		571	1059	4526
8050.212	4		1406	1065	5417
8063.187	3		947	979	2246
8278.313	3		369	979	4541
8350.185	4		1075	1093	4817
8377.052	6		586	1326	9606
8390.938	6		1018	1316	6092
8405.273	8		530	1632	21332
8435.438	8		6170	1538	7231
8449.776	8		1111	1605	10370
8492.053	20		1660	3096	43704
8505.991	58		1012	7975	105570
8521.880	25		1198	3737	41755
8543.596	13		1097	2206	12961
8561.837	25		1097	3719	42537
8578.478	16		927	2552	28785
8594.712	12		971	2131	17767
8605.718	14		1300	2314	18465
8616.877	12		693	2110	21315
8633.398	12		907	2130	19795
8648.962	8		863	1657	12023
8662.430	9		1225	1674	13021
8673.960	9		386	1678	20236
8700.404	6		937	1331	8862
8714.628	7		1012	1474	12527
8727.593	6		1145	1313	7919
8738.330	6		1808	1292	5873

Figure 3-2. (A) HPLC purification and (B) Mass of IGF-DOPA.

3.3.2 Binding assay

The binding activity of IGF-DOPA to polystyrene and titanium was confirmed using QCM-D (Figure 3-3). A wild type IGF-1 was used as a negative control. IGF-DOPA indicated high binding activity to polystyrene and titanium surface, but the wild type IGF-1 indicated very low or almost no binding activity to these surfaces. The enhanced binding activity of IGF-DOPA on material surfaces was considered to be due to the reaction between the amine groups of lysines with the catechol groups of DOPA. The reaction of catechol group of DOPA with amino group of lysine side in the peptide was considered to lead thin layer formation on organic and inorganic material surfaces.

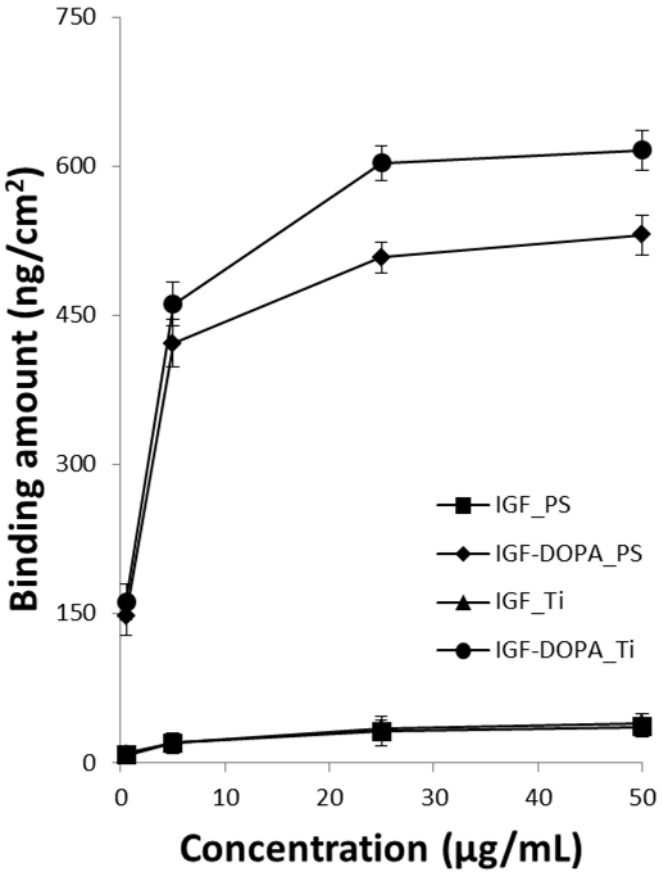

Figure 3-3. Binding assay of IGF and IGF-DOPA on polystyrene (PS) and titanium (Ti) surfaces. Mean ± S.D. n=3.

3.3.3 Biological activity of immobilized IGF-DOPA

Cell proliferation activity of IGF-DOPA was investigated by CCK-8 assay (Figure 3-4). Figure 3-4 shows NIH/3T3 cell growth on polystyrene and titanium plates treated with IGF-1 or IGF-DOPA. The initial number of cells seeded was taken as 100%. IGF-DOPA bound on the surfaces was found to be more active than free IGF on both surfaces. This result was considered to be caused by the high local concentration and multivalent immobilization of IGF moiety on surface.

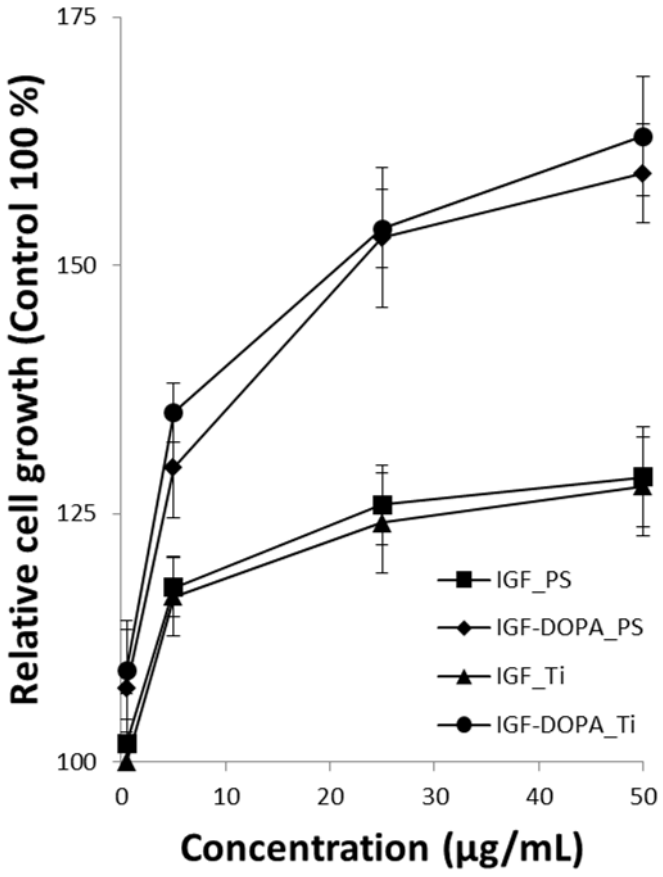

Figure 3-4. Cell proliferation on polystyrene (PS) and titanium (Ti) surfaces treated with free IGF or IGF-DOPA, respectively. Mean ± S.D. n=3.

The differentiation of MC3T3-E1 cell was observed by western blot (Figure 3-5) and Alizarin Red S staining (Figure 3-6). Osteogenesis can be monitored by some markers such as osteopontin and osteocalcin. After 14 days, IGF-DOPA promoted cell differentiation more effectively than water soluble IGF-1.

Alizarin Red S staining was also used to confirm calcium deposition during cell differentiation. The calcification area in the cells was shown as red stained pattern. After 14 days, almost no stained area was detected in the cells without IGF-1. However, cultured cells on IGF-DOPA-treated titanium surface showed larger stained area than that on IGF-treated surface (Figure 3-6(A)). Alizarin Red S stained level was quantified by absorbance measurement of extract and the result is shown in Figure 3-6(B). The absorbance from the cell extract on IGF-DOPA-immobilized surface shows higher value than that on IGF-treated surface. The result demonstrated that the cell differentiation was accelerated by immobilization of IGF-DOPA.

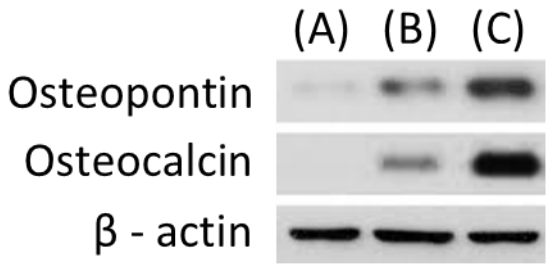

Figure 3-5. Western blot analysis of osteogenic markers osteopontin and osteocalcin. MC3T3-E1 cell was cultured for 14 days (A) on titanium (Ti), (B) in the presence of soluble IGF on Ti, and (C) in the presence of IGF-DOPA on Ti.

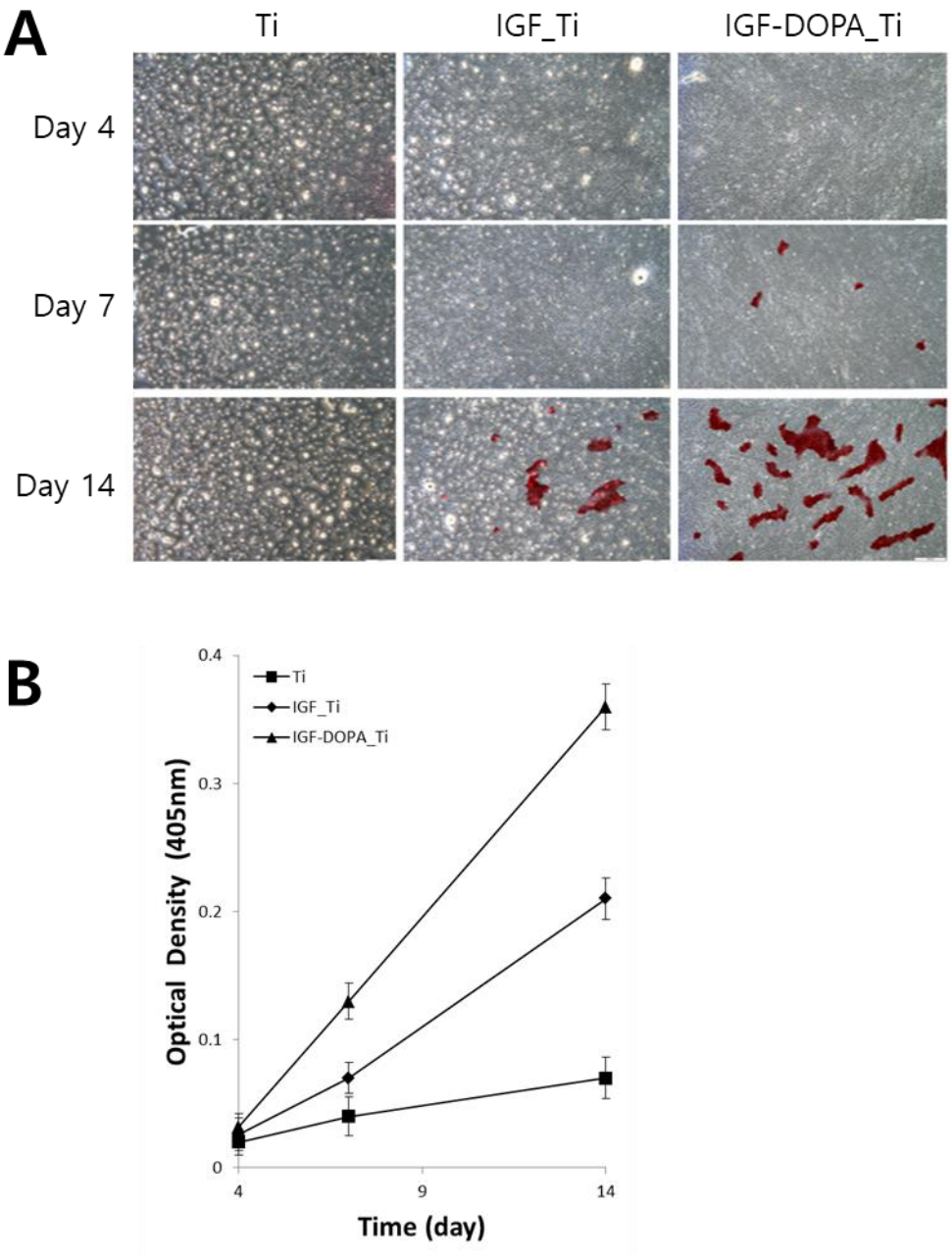

Figure 3-6. Cell differentiation on IGF or IGF-DOPA-treated titanium (Ti) surfaces. (A) Alizarin Red S stained images. (B) Quantification of Alizarin Red S stained levels. Mean ± S.D. n=3.

3.4 Conclusion

IGF-1 containing DOPA was designed by inspired from the underwater adhesive mussel protein. The prepared IGF-DOPA showed strong binding activity to various material surfaces such as polystyrene and titanium. The IGF-DOPA immobilized surface promoted cell proliferation and differentiation more efficiently than free IGF-1 through activation of cell signal transduction. Therefore, the design of growth factor with DOPA peptide is useful for binding growth factor for modification of biomaterial surfaces.

3.5 References

1. D.M. Monti, D. Guarnieri, G. Napolitano, R. Piccoli, P. Netti, S. Fusco, A. Arciello, Biocompatibility, uptake and endocytosis pathways of polystyrene nanoparticles in primary human renal epithelial cells, *Journal of Biotechnology*, 193, 3-10, 2015.

2. Y. Wang, H. Yu, C. Chen, Z. Zhao, Review of the biocompatibility of micro-arc oxidation coated titanium alloys, *Materials & Design*, 85, 640-652, 2015.

3. J. Low, B. Cheng, J. Yu, Surface modification and enhanced photocatalytic CO_2 reduction performance of TiO_2: a review, *Applied Surface Science*, 392, 658-686, 2017.

4. D.J. Miller, D.R. Dreyer, C.W. Bielawski, D.R. Paul, B.D. Freeman, Surface modification of water purification membranes, *Angewandte Chemie International Edition*, 56, 4662-4711, 2017.

5. J. Wen, X. Li, W. Liu, Y. Fang, J. Xie, Y. Xu, Photocatalysis fundamentals and surface modification of TiO_2 nanomaterials, *Chinese Journal of Catalysis*, 36, 2049-2070, 2015.

6. Y. Chen, Y. Xianyu, X. Jiang, Surface modification of gold nanoparticles with small molecules for biochemical analysis, *Accounts of Chemical Research*, 50, 310-319, 2017.

7. M.L. Amin, J.Y. Joo, D.K. Yi, S.S.A. An, Surface modification and local orientations of surface molecules in nanotherapeutics, *Journal of Controlled Release*, 207, 131-142, 2015.

8. L.D. Sánchez, N. Brack, A. Postma, P.J. Pigram, L. Meagher, Surface modification of electrospun fibres for biomedical applications: a focus on radical polymerization methods, *Biomaterials*, 106, 24-45, 2016.

9. P.K. Forooshani, B.P. Lee, Recent approaches in designing bioadhesive materials inspired by mussel adhesive protein, *Journal of Polymer Science Part A: Polymer Chemistry*, 55, 9-33, 2017.

10. C.F. Huang, Surface-initiated atom transfer radical polymerization for applications in sensors, non-biofouling surfaces and adsorbents, *Polymer Journal*, 48, 341, 2016.

11. K. Shi, J. Li, Z. Cao, P. Yang, Y. Qiu, B. Yang, Y. Wang, Y. Long, Y. Liu, Q. Zhang, A pH-responsive cell-penetrating peptide-modified liposomes with active recognizing of integrin αvβ3 for the treatment of melanoma, *Journal of Controlled Release*, 217, 138-150, 2015.

12. N. Reznikov, J. Steele, P. Fratzl, M. Stevens, A materials science vision of extracellular matrix mineralization, *Nature Reviews Materials*, 1, 16041, 2016.

13. J. Britton, C.L. Raston, G.A. Weiss, Rapid protein immobilization for thin film continuous flow biocatalysis, *Chemical Communications*, 52, 10159-10162, 2016.

14. D. Chen, L. Zhao, W. Hu, Protein immobilization and fluorescence quenching on polydopamine thin films, *Journal of Colloid and Interface Science*, 477, 123-130, 2016.

15. D.M. Ornitz, N. Itoh, The fibroblast growth factor signaling pathway, *Wiley Interdisciplinary Reviews: Developmental Biology*, 4, 215-266, 2015.

16. H. Kato, Y. Sekine, Y. Furuya, Y. Miyazawa, H. Koike, K. Suzuki, Metformin inhibits the proliferation of human prostate cancer PC-3 cells via the downregulation of insulin-like growth factor 1 receptor, *Biochemical and Biophysical Research Communications*, 461, 115-121, 2015.

17. V.S. Cortez, L. Cervantes-Barragan, M.L. Robinette, J.K. Bando, Y. Wang, T.L. Geiger, S. Gilfillan, A. Fuchs, E. Vivier, J.C. Sun, Transforming growth factor-β signaling guides the differentiation of innate lymphoid cells in salivary glands, *Immunity*, 44, 1127-1139, 2016.

18. P. Sivashankari, M. Prabaharan, Prospects of chitosan-based scaffolds for growth factor release in tissue engineering, *International Journal of Biological Macromolecules*, 93, 1382-1389, 2016.

19. S.J. Lee, D. Lee, T.R. Yoon, H.K. Kim, H.H. Jo, J.S. Park, J.H. Lee, W.D. Kim, I.K. Kwon, S.A. Park, Surface modification of 3D-printed porous scaffolds via mussel-inspired polydopamine and effective immobilization of rhBMP-2 to promote osteogenic differentiation for bone tissue engineering, *Acta Biomaterialia*, 40, 182-191, 2016.

20. D.W. Song, S.H. Kim, H.H. Kim, K.H. Lee, C.S. Ki, Y.H. Park, Multi-biofunction of antimicrobial peptide-immobilized silk fibroin nanofiber membrane: implications for wound healing, *Acta Biomaterialia*, 39, 146-155, 2016.

21. J. Shang, H. Liu, C. Qi, K. Guo, V.C. Tran, Evaluation of curing and thermal behaviors of konjac glucomannan–chitosan–polypeptide adhesive blends, *Journal of Applied Polymer Science*, 132, 42202, 2015.

22. M.A. Gonzalez, J.R. Simon, A. Ghoorchian, Z. Scholl, S. Lin, M. Rubinstein, P. Marszalek, A. Chilkoti, G.P. López, X. Zhao, Strong, tough, stretchable, and self-adhesive hydrogels from intrinsically unstructured proteins, *Advanced Materials*, 29, 1604743, 2017.

23. W. Wei, L. Petrone, Y. Tan, H. Cai, J.N. Israelachvili, A. Miserez, J.H. Waite, An underwater surface-drying peptide inspired by a mussel adhesive protein, *Advanced Functional Materials*, 26, 3496-3507, 2016.

24. M.A. North, C.A. Del Grosso, J.J. Wilker, High strength underwater bonding with polymer mimics of mussel adhesive proteins, *ACS Applied Materials & Interfaces*, 9, 7866-7872, 2017.

25. L. Li, H. Zeng, Marine mussel adhesion and bio-inspired wet adhesives, *Biotribology*, 5, 44-51, 2016.

26. B.K. Ahn, Perspectives on mussel-inspired wet adhesion, *Journal of the American Chemical Society*, 139, 10166-10171, 2017.

27. S. Ates, E. Zor, I. Akin, H. Bingol, S. Alpaydin, E.G. Akgemci, Discriminative sensing of DOPA enantiomers by cyclodextrin anchored graphene nanohybrids, *Analytica Chimica Acta*, 970, 30-37, 2017.

28. F. Scognamiglio, A. Travan, I. Rustighi, P. Tarchi, S. Palmisano, E. Marsich, M. Borgogna, I. Donati, N. de Manzini, S. Paoletti, Adhesive and sealant interfaces for general surgery applications, *Journal of Biomedical Materials Research Part B: Applied Biomaterials*, 104, 626-639, 2016.

29. A.C. Sandberg-Nordqvist, P.A. Stahlhom, M. Reinecke, V.P. Collins, H.V. Holst, V. Sara, Characterization of Insulin-like Growth Factor 1 in Human Primary Brain Tumors, *Cancer Research*, 53, 2475-2478, 1993.

30. D.R. Van Lonkhuyzen, B.G. Hollier, G.K. Shooter, D.I. Leavesley, Z. Upton, Chimeric vitronectin: insulin-like growth factor proteinsenhance cell growth and migration through co-activation of receptors, *Growth Factors*, 25, 295-308, 2007.

31. G.L. Francis, F.M. Upton, F.J. Ballard, K.A. McNeil, J.C. Wallace, Insulin-like growth factors 1 and 2 in bovine colostrum. Sequences and biological activities compared with those of a potent truncated form, *Biochemical Journal*, 251, 95-103, 1988.

32. B.P. Lee, P.B. Messersmith, J.N. Israelachvili, J.H. Waite, Mussel-inspired adhesives and coatings, *Annual Reviews of Materials Research*, 41, 99-132, 2011.

CHAPTER 4

CONCLUSIONS

4.1 Summary

This thesis described the development and design of IGF-1 for its application in strategies of accelerating cell growth and adhesion. Two strategies involving the use of photo-reactive alginate and underwater adhesive mussel protein were discussed in detail.

In **Chapter 1**, a general background was presented related to the research work. This chapter contained the background information, application techniques, and methods used for the study in this thesis.

In **Chapter 2**, the furfuryl group is reported to be successfully introduced into alginate. Two photosensitizers showed similar photo-gelation ratios. The amount of formed gel monotonously increased with the increase of exposure time and the increase of concentration and molecular weight of furfuryl alginate. The high gel formation ratio was considered to result from the high content of furan in the alginate. It was concluded that the content of crosslinking point furan determined the gel formation efficiency. The photo-crosslinked F-Alginate slowly released incorporated molecules. The molecular weight effect was observed on the release behavior of the molecules, and small molecules were quickly released from the gel. F-Alginate released the molecules by the simple diffusion similar to the conventional alginate hydrogels. The cytotoxicity of F-Alginate was negligible. Cell growth was enhanced in the presence of IGF-1-incorporated F-Alginate. Because of these reasons, visible light-curable F-Alginate effectively encapsulates the bioactive molecules to achieve a sustained-release effect on cells for the improvement of proliferation and differentiation.

Chapter 3 presents the synthesis of mussel-inspired IGF-DOPA to enhance cell growth at the surface of polystyrene and titanium. DOPA is an important compound in the composition of marine adhesive proteins, such as these found in

mussels. IGF-DOPA was prepared using solid-phase peptide synthesis, conjugating the truncated IGF-1 and DOPA-Lys-DOPA-Lys-DOPA-Gly. The binding of IGF-DOPA on polystyrene and titanium surface was investigated using QCM-D. IGF-DOPA could successfully bind to surfaces, whereas the wild-type IGF-1 could not. In terms of cell proliferation and differentiation, IGF-DOPA also returned higher cell activity than the wild-type IGF-1. In conclusion, photo-reactive alginate for IGF-1 release and IGF-DOPA successfully demonstrated the enhancement of cell growth and adhesion. These designed materials can be used for efficient future biomaterials, such as drug delivery and surface modification.

4.2 Future directions

When delivering growth factors to enhance tissue regeneration, the major obstacle is obtaining optimal gradients and concentrations of the suitable growth factors for precise requirements. Thus far, there has been substantial progress in understanding fundamental information about the biological properties of growth factors and the microenvironment to further make more effective growth factor-based delivery systems for the control of protein delivery. A wide variety of approaches, such as covalent conjunctions, nanoparticle (NP)-based delivery systems, and ECM-inspired binding, have been used in recent decades to facilitate tissue repair. Most delivery systems showed in this research demonstrated therapeutic potential and enhanced stability of the growth factors upon immobilization when compared to drug delivery systems and traditional regenerative medicine.

4.2.1 Approach for efficient delivery of growth factors

A major hindrance to efficient delivery of growth factors for medical use is that significant amounts of biomolecules are required during tissue regeneration. The controlled growth factor presentation will continue to play an important role in tissue engineering approaches, and it will be conjugated with biomaterials that permit controllable release profiles to achieve regulation during delivery. For this strategy to realize its vast potential, continued efforts to understand biological signaling pathways during tissue development are required. This requirement involves recapitulating the concentrations and distributions of bioactive growth factors during those processes accounting for the effects of cell and carriers on target cells. Such knowledge could use engineering design to specifically guide the release of growth factor from the delivery system. Thus, the delivery system would not only release the appropriate growth factors but also offer visions on growth factors and microenvironments during tissue regeneration in vivo. If these factors are considered, the various growth factors can hold excellent promise for future therapies in medical regenerative medicine.

Growth factor delivery from various biomaterials has offered satisfactory results in fibular demerit and bone fractures, improvements in periprosthetic fractures and Alzheimer’s disease, and advances in dermal healing, skeletal muscle regeneration, and peripheral nerve regeneration. The important advances have optimized the delivery of growth factors to target tissues and have demonstrated their progression through clinical demonstrations to be considered suitable for commercial use. However, the high amount of growth factors are required for therapeutic benefit, and in some cases, systemic exposure of these amounts has caused certain side effects, including increased wound complications, ectopic tissue formation, cancer risk, or radiculopathy.

4.2.2 Combination of growth factors

For efficient delivery of growth factors, it is evident that further research is necessary regarding smart biomaterial designs and programmable release of growth factor delivery. Combining growth factors (TGF/IGF, BMP/VEGF) and their release profiles using different biomaterials has the potential to enhance tissue regeneration *in vivo*. Therefore, multiple release of a growth factor plays an important role in the proliferation, recruitment, and functional activities of cells during the promotion of tissue regeneration and the early stages of wound repair. Second, while many growth factors have been confirmed as efficient at high doses in biomedical applications, the need for precise and safe medical treatments has driven the research toward the study of novel delivery systems and optimization of the concentrations of the right growth factors. Thus, biomaterials that are sensitive to exogenous stimuli have been widely applied to deliver growth factors. Indeed, the development of biomaterials is expected to provide an attractive alternative for delivering the various growth factors in a better-regulated manner in the future.

4.3 Conclusions and perspectives

As studies on tissue regeneration converge on acknowledging the need for a multifunctional approach to better reenact the complex process of tissue repairing, combinations of appropriate biomaterial carriers with bioactive proteins will direct innovation. Until present, biomaterial–growth factor complex delivery systems using natural or synthetic materials in various structures have supplied efficient differential immobilization and release, which has enabled the effective release of growth factors with biological activity in the local environment. These new methods of biomaterial preparation are still in the initial approach of development and research and lack consistent clinical data. Future studies on the use of biomaterials in tissue regeneration

and repair should be focused on an expansive understanding of tissue–biomaterial interactions and the optimization of their chemical and physical properties for long-term performance. Thus, the synthesis of biomaterials in terms of biocompatibility and structural compositions that mimic tissue repair through the combination of multiple areas, including biological and chemical stimuli (such as adhesive proteins, growth factors, or functional groups) and physical conditions (micro/nano-particles, stimuli-responsive property, shear stress, and hydrophilic and hydrophobic properties), is significant for the research of next-generation biomedical device. Finally, the potential of growth factor-based delivery systems for medical use strongly depends on more researches and approaches that combine biomaterials, medicine, engineering, and the technical knowledge of medical researches. Close cooperation among specialists in tissue engineering, materials science, medicine, and chemistry may eventually reduce the latency between current research and clinical application, and it is likely that growth factor delivery approaches will offer many therapeutic benefits in the therapy of complex wounds in the near future.

Acknowledgments

This doctoral dissertation is a compilation of the research carried out at Emergent Bioengineering Materials Research Team, RIKEN during 2015–2019.

First, I would like to thank and gratitude to advisor Professor Yoshihiro Ito for giving me the nice opportunity of pursuing Ph.D at Tokyo Institute of Technology. I am grateful for his scientific support, professional guidance, constructive criticism, and encouragement during the research. I am fortunate to have worked in his laboratory.

I express my gratitude to Professor Eiry Kobatake for his friendly demeanor and optimistic supervision in supporting my research. He always helped me with my research and solved problems. I also appreciate Professor Tae-Il Son, who worried and cared for me and helped me.

I really thank Dr. Takanori Uzawa, my mentor. His advice was very useful. He always brought scientific and logical perspectives. I am deeply impressed by his advice. I would also like to thank Dr. Seiichi Tada who was a part of discussions and solving problems. Many thanks to Dr. Jun Akimoto for being generous and supporting me in the research. I have learned a lot from him.

Thanks to my dear friends Sung-Min Kim, Kon Son, Il-Jae Min, Eun-Hye Kim, So-Jung Park, Roopa Dharmatti, Chinmay Phadke, Stefan Mueller, Ren Xueli, MA Karimi, and Masyh Saber who made me enjoy my life. I also appreciate the help of Ms. Kyoko Yamanaka.

Special gratitude to my parents, Mr. Jung-Il Heo and Ms. Won-Choon Chang, who always supported my education morally and financially. In addition, thanks to my younger sister, Yu-Ri Heo, for her encouragement. I appreciate the support by Junior Research Associate (JRA) program for graduate students at RIKEN.

Finally, thank you to all of the lab members and mentors who gave their time and provided me with insight into their experience with RIKEN life.

List of Publications

1. Y. Heo, J. Akimoto, E. Kobatake, Y. Ito, Gelation and release behavior of visible light-curable alginate, *Polymer Journal*, published, 30 October 2019.
2. S. Tada, H. Mao, Y. Heo, X. Ren, SH. Park, T. Isoshima, L. Zhu, X. Zhou, R. Ito, S. Kurata, M. Osaki, S. Tsuneda, E. Kobatake, Y. Ito, Gene-expression control surfaces by mussel-inspired adhesive growth factors, under preparation